

137

NOV 1985

CONTRACTOR REPORT

SAND83-7068
Unlimited Release
UC-70

Lining Considerations for a Circular Vertical Shaft in Generic Tuff

William Hustrulid
Mining Engineering Consultant
28599 Buchanan Drive
Evergreen, CO 80439

Prepared by Sandia National Laboratories Albuquerque, New Mexico 87185
and Livermore, California 94550 for the United States Department of Energy
under Contract DE-AC04-76DP00789

Printed December 1984

Issued by Sandia National Laboratories, operated for the United States Department of Energy by Sandia Corporation.

NOTICE: This report was prepared as an account of work sponsored by an agency of the United States Government. Neither the United States Government nor any agency thereof, nor any of their employees, nor any of their contractors, subcontractors, or their employees, makes any warranty, express or implied, or assumes any legal liability or responsibility for the accuracy, completeness, or usefulness of any information, apparatus, product, or process disclosed, or represents that its use would not infringe privately owned rights. Reference herein to any specific commercial product, process, or service by trade name, trademark, manufacturer, or otherwise, does not necessarily constitute or imply its endorsement, recommendation, or favoring by the United States Government, any agency thereof or any of their contractors or subcontractors. The views and opinions expressed herein do not necessarily state or reflect those of the United States Government, any agency thereof or any of their contractors or subcontractors.

Printed in the United States of America
Available from
National Technical Information Service
U.S. Department of Commerce
5285 Port Royal Road
Springfield, VA 22161

NTIS price codes
Printed copy: A04
Microfiche copy: A01

SAND83-7068

Unlimited Release
Printed December 1984

LINING CONSIDERATIONS FOR A CIRCULAR
VERTICAL SHAFT IN GENERIC TUFF

by

William Hustrulid

for

Sandia National Laboratories
P.O. Box 5800
Albuquerque, New Mexico 87185

Under Sandia Contract: 50-1555

Sandia Contract Monitor
G. Kenton Beall
Geotechnical Design Division

ABSTRACT

This report summarizes some of the classical formulas used in the design of concrete linings for vertical, circular bored shafts and applies them to a generic shaft in tuff. The lining requirements are shown to be highly dependent on the rock mass strength and in situ stress field. For a given stress field, the required lining thickness is analyzed as a function of rock mass strength, which is approximated by various fractions of the laboratory strength. For the cases considered, if the rock mass strength is equal to the laboratory compressive strength, then no lining would be required. If the strength reduction factor is 2, a concrete lining (compressive strength = 35 MPa) having a thickness of 0.3 m would provide a safety factor of at least 1.5. For larger strength reduction factors, the required lining thickness in the different formations is quite variable. An analysis of measured lining pressures for the conventionally sunk (excavated with explosives) Mt. Taylor shaft (Grants, New Mexico) has been included. The results suggest that a substantial damaged (relaxed) zone was created during the excavation process. The lining pressures are much less than would be predicted under the assumption of no damage. Therefore, the recommendations presented in this report would have to be modified for application to conventionally sunk, rather than bored, shafts. The approach described and the equations presented may, it is believed, be used with care to analyze different generic shaft scenarios. However, high priority should be placed on obtaining the best estimates possible for rock mass strength and an in situ stress field.

CONTENTS

	<u>Page</u>
Abstract	i
1.0 Introduction	1
2.0 Problem Definition	3
3.0 Technical Approach	7
3.1 Strictly Elastic Zone	7
3.2 Elastic Zone Material Properties Equal Plastic Zone Material Properties	17
3.3 Elastic Zone Material Properties Do Not Equal Plastic Zone Material Properties	22
4.0 Shaft Lining Analysis	25
4.1 Introduction	25
4.2 Example of Rock Stiffness Calculation	29
4.3 Example of Lining Stiffness Calculation	33
4.4 Lining Selection for the Generic Tuff Shaft	35
5.0 Analysis of the Data From the Mt. Taylor Shaft	41
6.0 Conclusions	47
7.0 Recommendations	49
8.0 References	51

LIST OF TABLES

<u>Table No.</u>	<u>Title</u>	<u>Page</u>
1	Rock Mass Characteristics at Depths Selected for Evaluation	3
2	K Values Assumed for Analysis and Resulting Stresses at the Shaft Wall	12
3	Matrix Strength Properties from Laboratory Measurements	12
4	Unconfined Compressive Strength and Tan β Values	13
5	Maximum Values of M Without Shaft Wall Failure	17
6	Radial Displacement (U_w) of the Shaft Wall as a Function of Applied Inner Pressure (P_i)	29
7	Radial Displacement (U_o) of the Outer Lining Wall as a Function of P_i Pressure (P_i)	34
8	Pressure Required to Prevent the Formation of a Relaxed Zone Around the Shaft	36
9	Contribution of Cohesion (ΔP) in Preventing Development of a Relaxed Zone Around the Shaft	38
10	Shaft Lining Pressures Developed in Cohesive Formations	38
11	Required Shaft Lining Thickness in Cohesive Formations (Safety Factor of 1.5)	39
12	Values Used for the Mt. Taylor Shaft Analysis	41
13	Measured and Expected Lining Pressures (P_i)	43
14	Maximum Shaft Lining Stresses	43
15	Predicted Radius and Thickness of the Relaxed Zone (R) Surrounding the Shaft	44
16	Rock Wall Movement Required to Achieve the Observed Lining Pressure Through Bulking	45
17	Maximum Lining Stresses as a Result of Full Bulking of the Relaxed Zone	45
18	Radial Displacement (U_o) of the Outer Shaft Wall Needed to Produce the P_i Observed Pressures	46

LIST OF FIGURES

<u>Figure No.</u>	<u>Title</u>	<u>Page</u>
1	Geometry and Coordinate System	4
2	Stresses at Shaft Wall--Horizontal ($r - \theta$) Plane	8
3	Mohr-Coulomb Failure Criterion Expressed in Terms of Shear and Normal Stresses	11
4	Mohr-Coulomb Failure Criterion Expressed in Terms of Principal Stresses	11
5	Stress-Strength Comparison for the Tuffaceous Beds (Calico Hills, 495 m)	14
6	Stress-Strength Comparison for the Bullfrog Layer	15
7	Stress-Strength Comparison for the Tram Layer	16
8	Diagrammatic Representation of the Plastic Zone Around a Shaft	19
9	Relationship Between Confining Pressure and Stress at Failure for Silty Mudstone	24
10	Lining Pressure--Radial Wall Displacement (for Equilibrium) for the Example Problem	30
11	Diagrammatic Representation of the Shaft Lining	31
12	Triaxial Compression Test Results, Mancos Shale Formation	42
13	Triaxial Compression Test Results, Upper Westwater Canyon Member of the Morrison Formation	42

1.0 INTRODUCTION

The work described in this report was performed for Sandia National Laboratories (SNL) as a part of the Nevada Nuclear Waste Storage Investigations (NNWSI) project. Sandia is one of the principal organizations participating in the project, which is managed by the U.S. Department of Energy's (DOE) Nevada Operations Office. The project is a part of the DOE's Terminal Storage program to safely dispose of the radioactive waste from nuclear power plants.

The DOE has determined that the safest and most feasible method currently known to dispose of such wastes is to emplace them in mined geologic repositories. The NNWSI project is conducting detailed studies of an area on and near the Nevada Test Site (NTS) in southern Nevada to determine the feasibility of developing a repository.

This investigation summarizes some of the pertinent rock mechanics theories dealing with the design of repository shafts and shaft linings. Equations are presented for a shaft in the following materials:

- strictly elastic (strength greater than the stresses);
- elastic-plastic zone formed near the shaft wall with a transition to elastic behavior at some radius, R ; the values of cohesion and angle of internal friction are the same in the elastic and plastic zones (as in sands or soil but not typical of rock);
- elastic-plastic zone formed near the shaft wall with a transition to elastic behavior at some radius, R ; the values of cohesion and angle of internal friction can be different in the plastic and elastic zones.

The extent of the plastic (broken) zone as a function of an applied pressure to the shaft wall has been characterized, and the amount of rock bulking as a function of damage zone extent also has been considered.

A number of investigators, including Westergaard (1907), Fenner (1938), Labasse (1949), Terzaghi (1943), Talobre (1957, 1967), Jaeger and Cook (1969), and Ladanyi (1974), have published equations regarding the behavior of rock in the vicinity of a vertical, circular shaft both with and without a lining. This report focuses on a review of the rock mechanics theory appropriate to application for shaft lining design, some initial calculations using properties of a generic tuff, and the results of an actual shaft lining project in soft rock.

2.0 PROBLEM DEFINITION

Complex analysis of the behavior of a vertical, circular shaft in generic tuff requires consideration of whether failure of the rock around the shaft is expected. The following conditions apply for all analyses:

- The shaft is drilled or bored (no excavation-induced damage zone).
- The shaft is circular and vertical.
- One of the principal stresses is vertical and is due to the weight of the overlying rock.
- The principal stresses in the plane normal to the shaft axis are equal. Horizontal field stress does not vary in magnitude with direction.
- The rock material obeys linear Mohr-Coulomb failure criteria.
- The geometry and coordinate system is as shown in Figure 1.

Equations are applied to a generic site in tuff. Three particular depths in the formations tested were chosen for evaluation as shown in Table 1 (Langkopf, 1982).

TABLE 1
ROCK MASS CHARACTERISTICS AT
DEPTHS SELECTED FOR EVALUATION

<u>Formation</u>	<u>Depth (m)</u>	<u>Stress Ratios (σ / σ)</u>	
		H	V
Tuffaceous Beds	495		0.87
Bullfrog	810		0.72
Tram	955		0.70

The vertical stress, which comes from the assumption of 25 kPa/m of depth, and is used often in rock mechanics to estimate the effects of overburden, was assumed to follow:

$$\sigma_v = 0.025 \text{ MPa/m} \times H \quad (1)$$

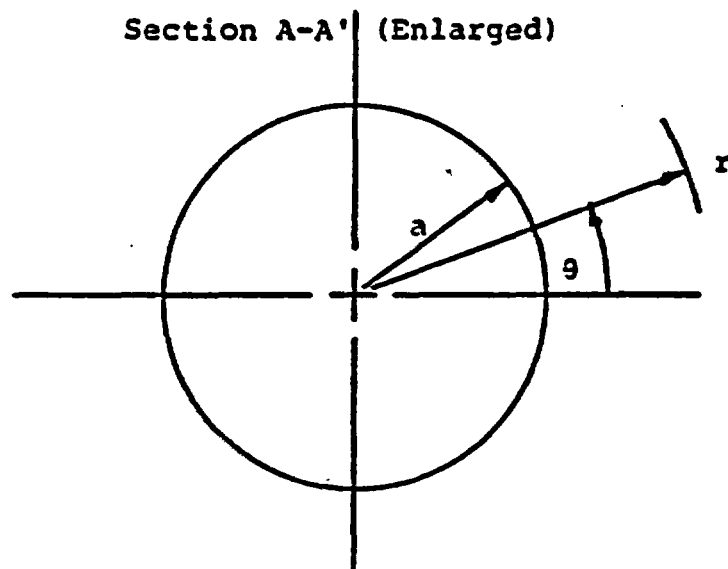
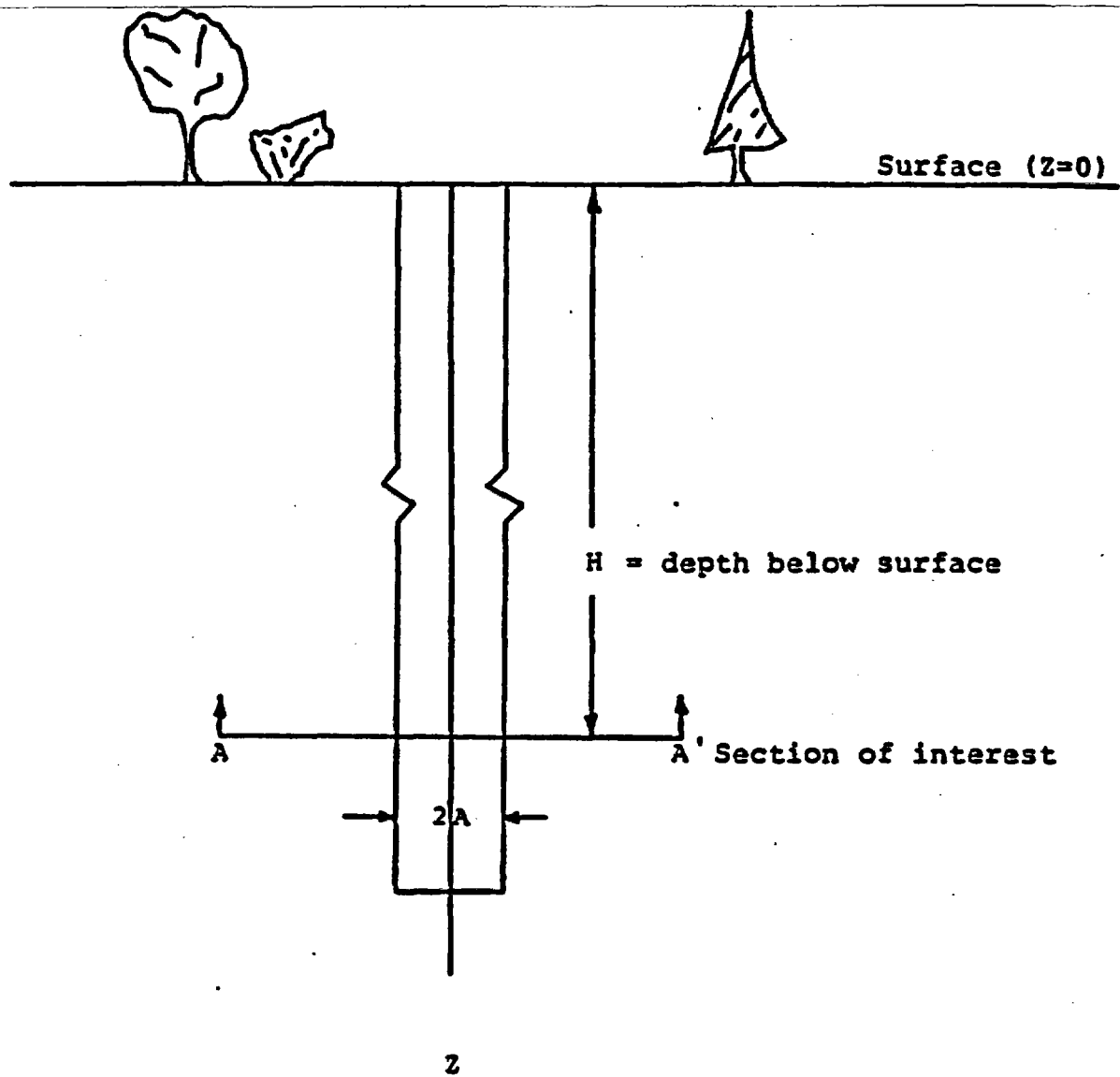


Figure 1. Geometry and Coordinate System

where

σ_v = overburden stress (MPa) and
H = depth (m).

The horizontal (σ_H) to vertical (σ_v) stress ratios presented in Table 1 were selected based upon the work of Langkopf (1982).

3.0 TECHNICAL APPROACH

3.1 Strictly Elastic Zone

For the purely elastic situation, two particular cases are considered:

Case 1: If (a) the ground is elastic, (b) the stresses are less than the strength of the rock, and (c) elastic displacement occurs before lining installation, the rock-induced stress on the lining would be zero and the thickness of the lining would be controlled by lining type and installation procedures.

Case 2: If conditions (a) and (b) of Case 1 apply but the lining is emplaced before the realization of full elastic wall displacement, then two possibilities exist:

- The shaft lining is installed with a gap of sufficient width between the rock wall and the outer shaft liner wall to preclude loading the shaft liner. The rock-induced stress on the lining would be zero and the thickness of the lining would be controlled by the lining type and installation procedures.
- No gap exists when the lining is installed. In this case, the lining is stressed to a degree, depending upon the rock and lining stiffness and the amount of elastic relaxation. (This case is addressed in Subsection 4.1.)

Case 1 is assumed to apply for the purposes of the following analysis.

The stresses in the rock surrounding the circular shaft (Figure 2) are given by

$$\begin{aligned} \sigma_z &= \sigma_v , \\ \sigma_\theta &= \sigma_H \left(1 + \frac{a^2}{r^2} \right) , \text{ and} \end{aligned} \tag{2}$$

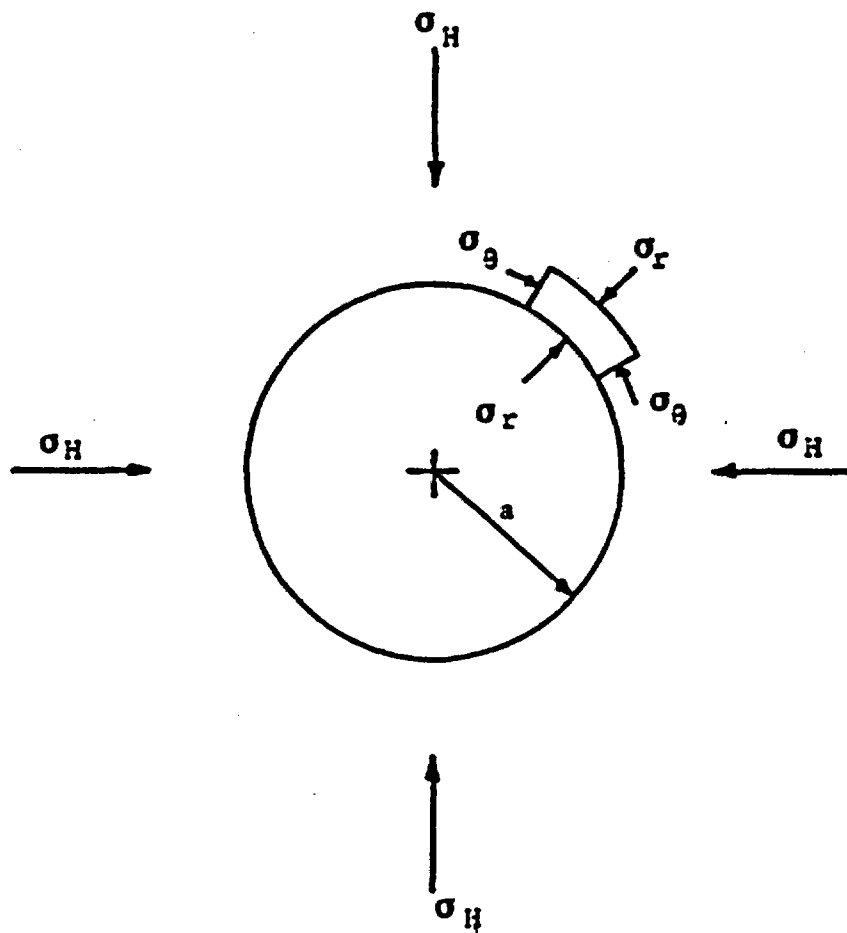


Figure 2. Stresses at Shaft Wall--Horizontal ($r - \theta$) Plane

$$\sigma_r = \sigma_H \left(1 - \frac{a^2}{r^2} \right), \quad (3)$$

where

$$\begin{aligned} \sigma_v &= \text{vertical field stress} = \gamma H, \\ \sigma_H &= \text{horizontal field stress} = K\gamma H, \\ H &= \text{depth below surface,} \\ \gamma &= \text{overburden stress/unit depth,} \\ K &= \text{factor relating the horizontal and vertical field stresses,} \\ a &= \text{shaft radius,} \\ r &= \text{distance measured from the center of the shaft,} \\ \sigma_z &= \text{principal stress in the vertical direction,} \\ \sigma_\theta &= \text{principal stress in the tangential direction, and} \\ \sigma_r &= \text{principal stress in the radial direction.} \end{aligned} \quad (4)$$

If the horizontal field stress is due to gravity alone,

$$K = \frac{\nu}{1 - \nu},$$

where ν = Poisson's ratio.

For typical values for rock of $\nu = 0.1$ to 0.5 , K varies between 0.11 and 1.0 . The potential for failure in the $r - z$ (vertical) plane would be examined when

$$K \leq 0.5 \quad (\sigma_z > \sigma_\theta > \sigma_r), \text{ and}$$

the potential for failure in the $r - \theta$ (horizontal) plane would be examined when

$$K > 0.5 \quad (\sigma_\theta > \sigma_z > \sigma_r).$$

When the horizontal field stress is due to other forces besides gravity, appropriate values of σ_H will be taken from measurements instead of calculating σ_H using Equation 4.

The equation for the envelope representing the Mohr-Coulomb failure criterion (Figure 3) is

$$\tau = c + \sigma \tan \phi \quad (5)$$

where

τ = shear strength,
 c = cohesion,
 σ = normal stress, and
 ϕ = angle of internal friction.

An alternative form of Equation 5 expressed in terms of the principal stresses, the unconfined compressive strength, and the passive pressure coefficient (Figure 4) is

$$\sigma_1 = \sigma_0 + \sigma_3 \tan \beta \quad (6)$$

where

σ_1 = maximum principal stress,
 σ_0 = unconfined compressive strength,
 σ_3 = minimum principal stress, and
 $\tan \beta$ = passive pressure coefficient.

Using the fact that

$$\sigma_0 = \frac{2c \cos \phi}{1 - \sin \phi} \quad \text{and}$$

$$\tan \beta = \frac{1 + \sin \phi}{1 - \sin \phi} \quad (7)$$

one can derive a third common form of the Mohr-Coulomb failure criterion:

$$\frac{\sigma_1 + c \cot \phi}{\sigma_3 + c \cot \phi} = \frac{1 + \sin \phi}{1 - \sin \phi}$$

Analysis of the rock strength under the stresses at the shaft wall ($r = a$) may predict whether failures will occur.

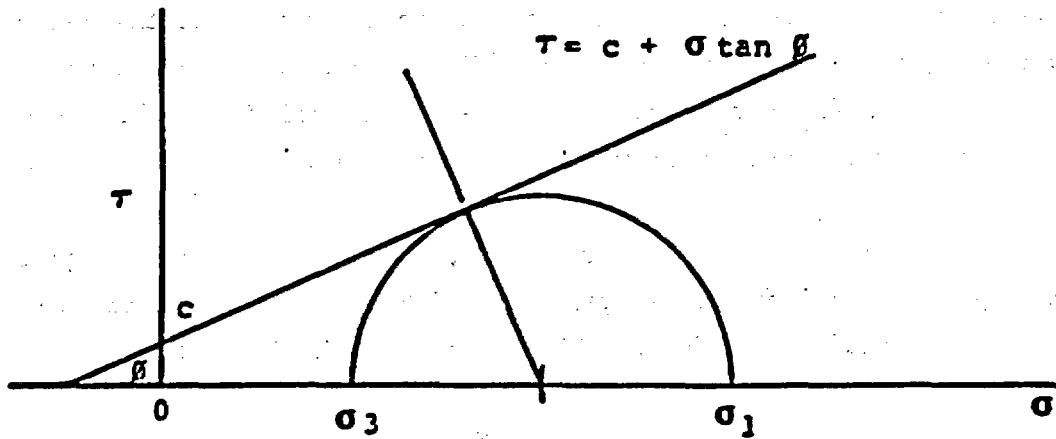


Figure 3. Mohr-Coulomb Failure Criterion Expressed in Terms of Shear and Normal Stresses

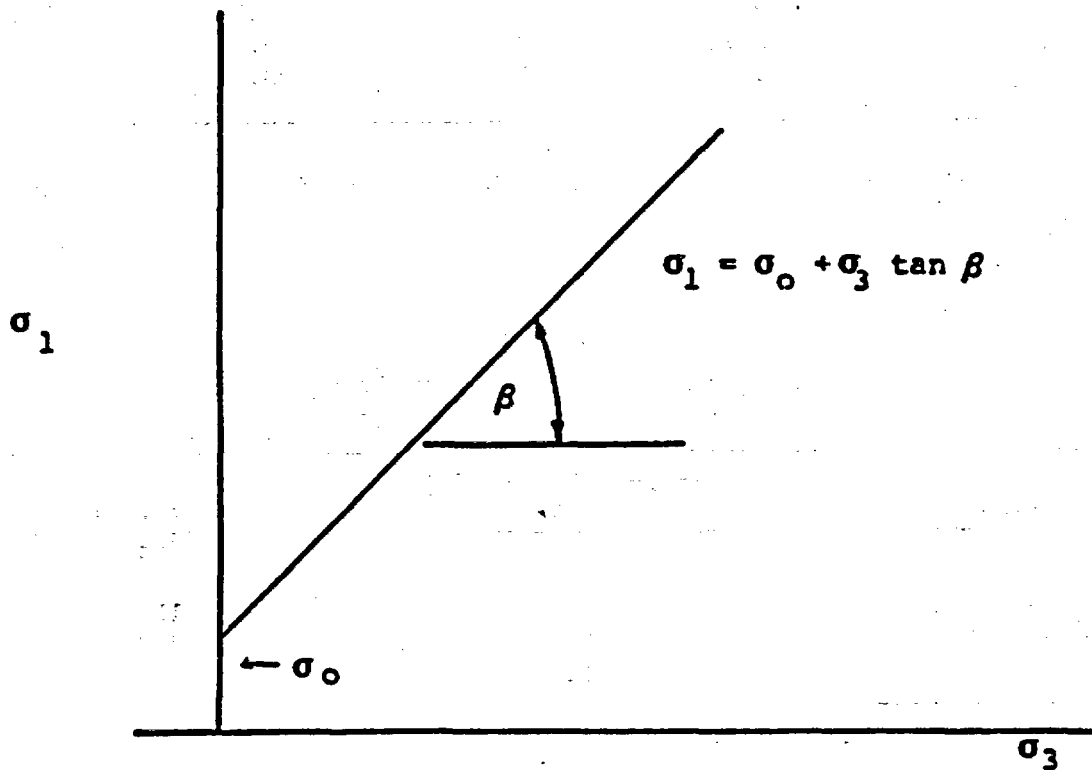


Figure 4. Mohr-Coulomb Failure Criterion Expressed in Terms of Principal Stresses

Initial field stress measurements (Langkopf, 1982) suggest that $K > 0.5$ ($K \approx 0.75$), and as a result, primary attention is focused on the behavior of the rock in the $r - \theta$ plane (Figure 2). From Equations 2 and 3, the maximum stress difference ($\sigma_\theta - \sigma_r$) occurs at the shaft wall ($\sigma_r = 0$). Therefore, the potential for failure is evaluated at that point.

If the average overburden stress, σ_v , is calculated using Equation 1, and the appropriate H values (depths from Table 1) and K values are considered, the stresses at the shaft wall are as shown in Table 2.

TABLE 2
K VALUES ASSUMED FOR ANALYSIS AND
RESULTING STRESSES AT THE SHAFT WALL

<u>Formation</u>	<u>K</u>	<u>Principal Stresses (MPa)</u>		
		<u>$\sigma_r = \sigma_3$</u>	<u>$\sigma_z = \sigma_2$</u>	<u>$\sigma_\theta = \sigma_1$</u>
Tuffaceous Beds	0.87	0	12.38	21.54
Bullfrog	0.72	0	20.25	29.16
Tram	0.70	0	23.88	33.43

The matrix strength properties for the relevant formations are given in Table 3.

TABLE 3
MATRIX STRENGTH PROPERTIES FROM
LABORATORY MEASUREMENTS^a

<u>Formation</u>	<u>Matrix Cohesion (c) (MPa)</u>	<u>Angle of Internal Friction (ϕ)</u>	
		<u>Wet</u>	<u>Dry</u>
Tuffaceous Beds	10	11°	25°
Bullfrog	12	25°	35°
Tram	12	25°	35°

^a Data are from Lappin, 1982.

From the values in Table 3 the unconfined compressive strength, σ_0 , and $\tan \beta$ can be calculated as shown in Table 4.

TABLE 4
UNCONFINED COMPRESSIVE STRENGTH AND TAN β VALUES

<u>Formation</u>	<u>Wet Properties</u>		<u>Dry Properties</u>	
	<u>σ_0 (MPa)</u>	<u>tan β</u>	<u>σ_0 (MPa)</u>	<u>tan β</u>
Tuffaceous Beds	24.11	1.47	31.34	2.47
Bullfrog	41.90	2.47	49.10	3.70
Tram	41.90	2.47	49.10	3.70

The corresponding strength curves for the three formations are given in Figures 5 through 7. The stresses at the shaft wall have been superimposed on the appropriate figures; the stresses lie below the strength curves, and if the laboratory properties are representative of the rock mass properties, no failure would result.

Unfortunately, rock mass strengths generally are considerably less than the strength of small core samples. (The laboratory tests were performed on cores 2.5 cm in diameter and 5.1 cm long.) The strength of soft materials can also deteriorate with time and in the presence of fluids. If the strength of the rock mass (S_{RM}) is related to the laboratory strength (S_{Lab}) by

$$S_{RM} = (1/M) S_{Lab} \quad , \quad \frac{1}{M} = \frac{S_{RM}}{S_{Lab}} \quad M = \frac{S_{Lab}}{S_{RM}} \quad (8)$$

the maximum values that M can assume without shaft wall failure can be calculated. The calculation of M for the Tuffaceous Beds is provided below as an example. The calculations are based on Equations 6 and 8.

Wet Strength

$$\sigma_1 = \sigma_\theta + \sigma_3 \tan \beta = S_{Lab} = 24.11 \text{ MPa}$$

where

$$\sigma_\theta = S_{RM} = 21.54 \text{ MPa (Table 2) and}$$

$$\sigma_3 = 0 \text{ (Table 2) .}$$

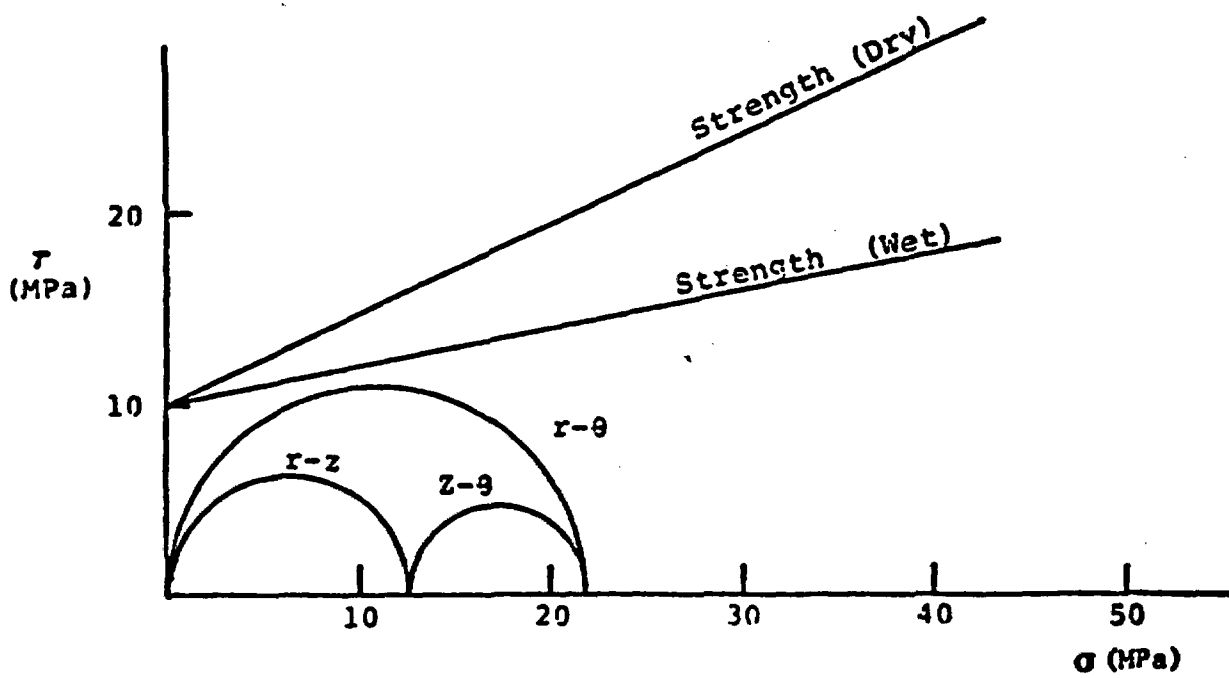
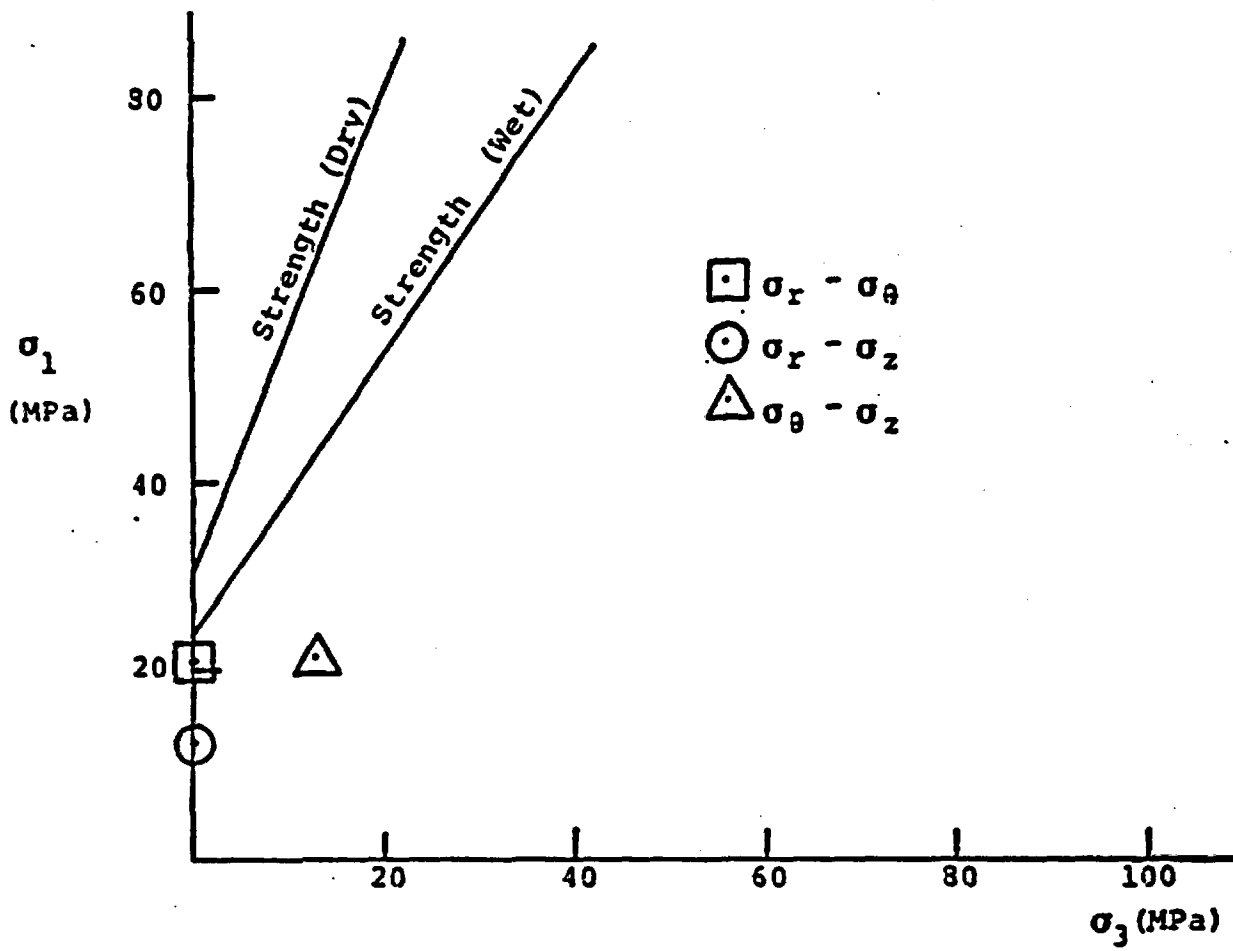


Figure 5. Stress-Strength Comparison for the Tuffaceous Beds (Calico Hills, 495 m)

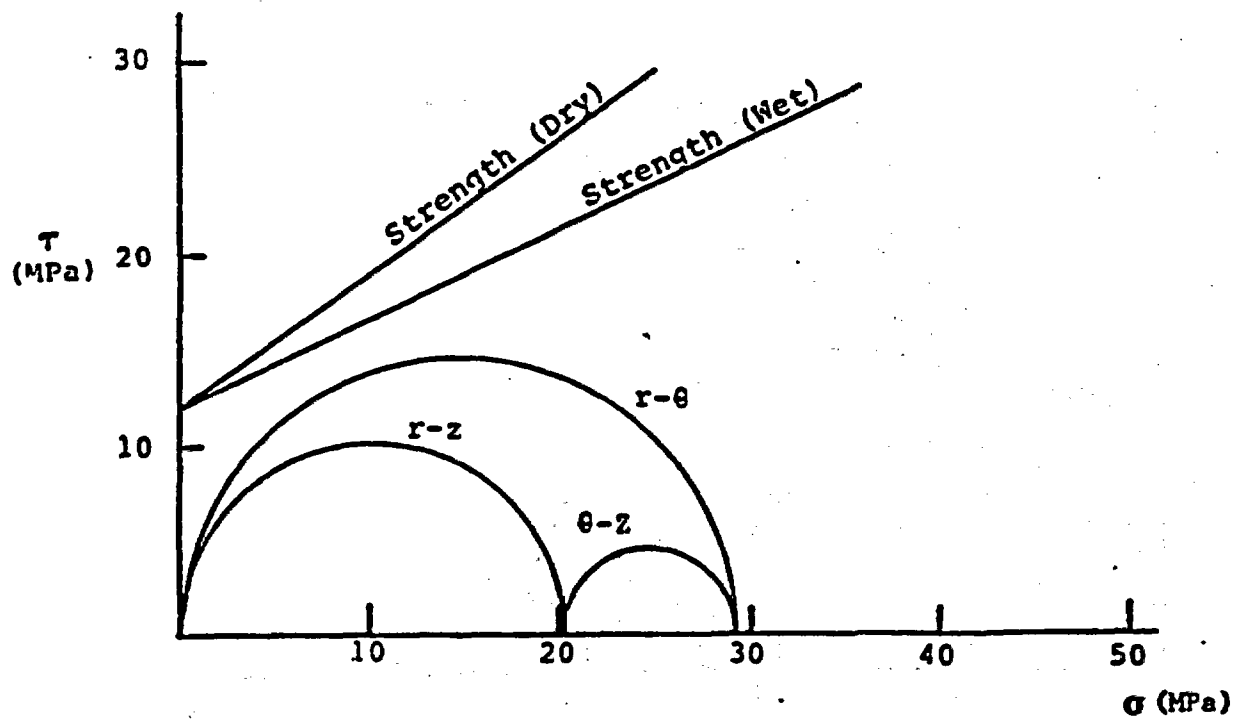
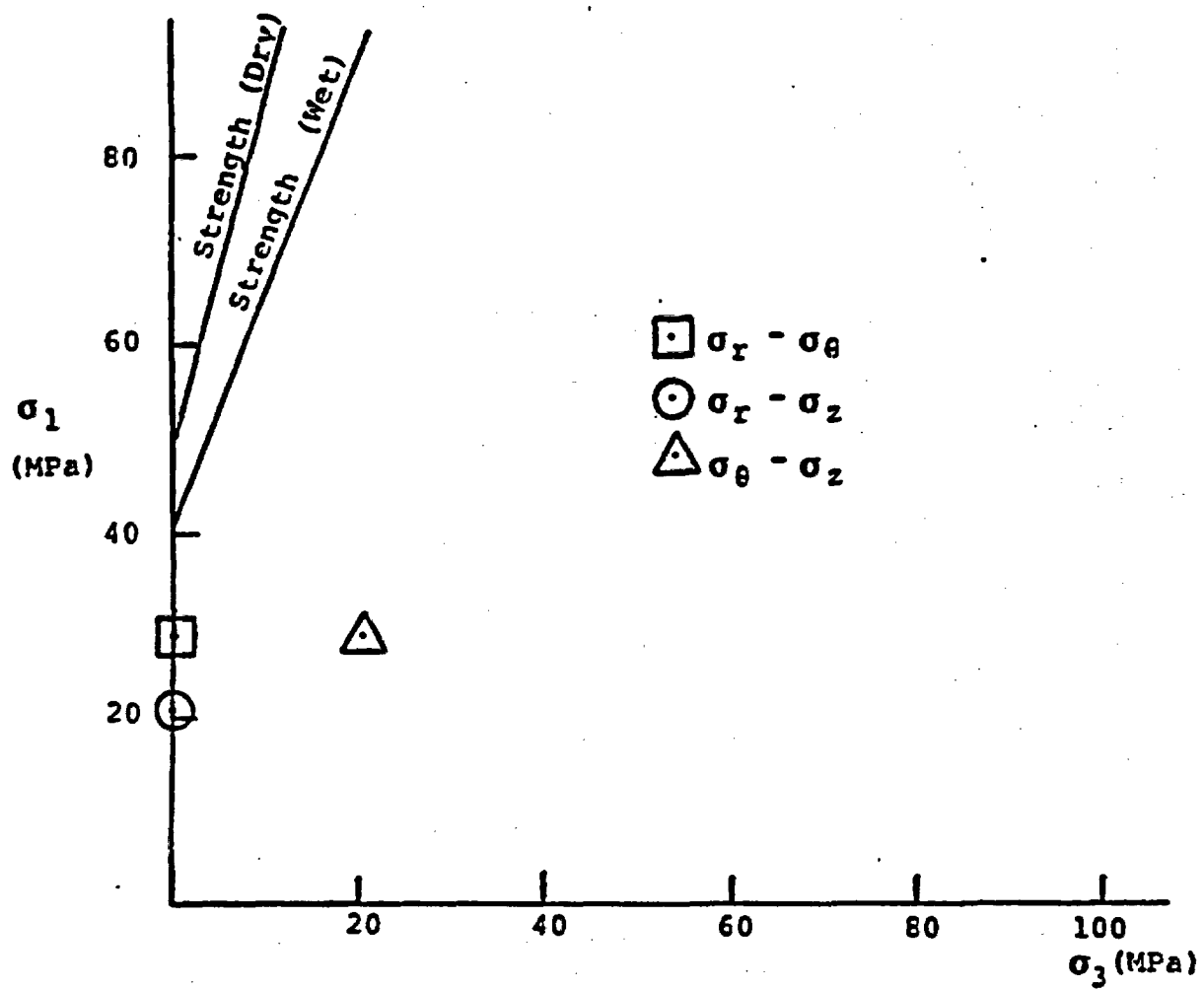


Figure 6. Stress-Strength Comparison for the Bullfrog Layer

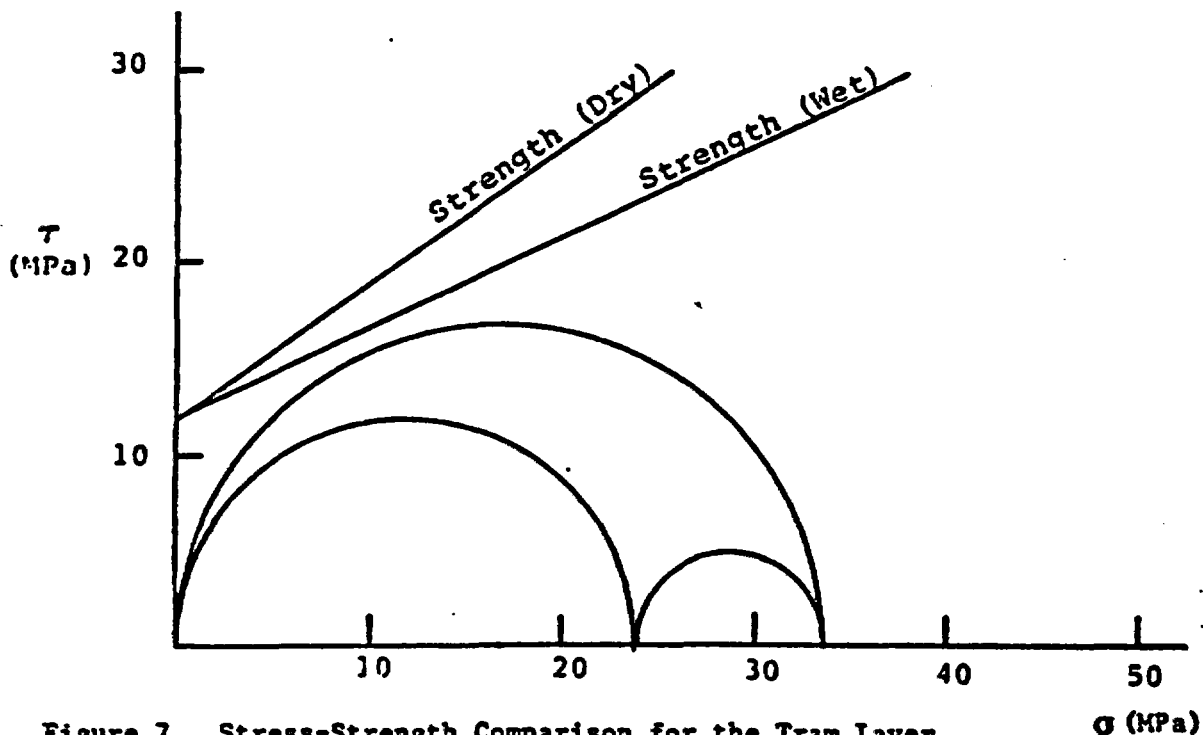
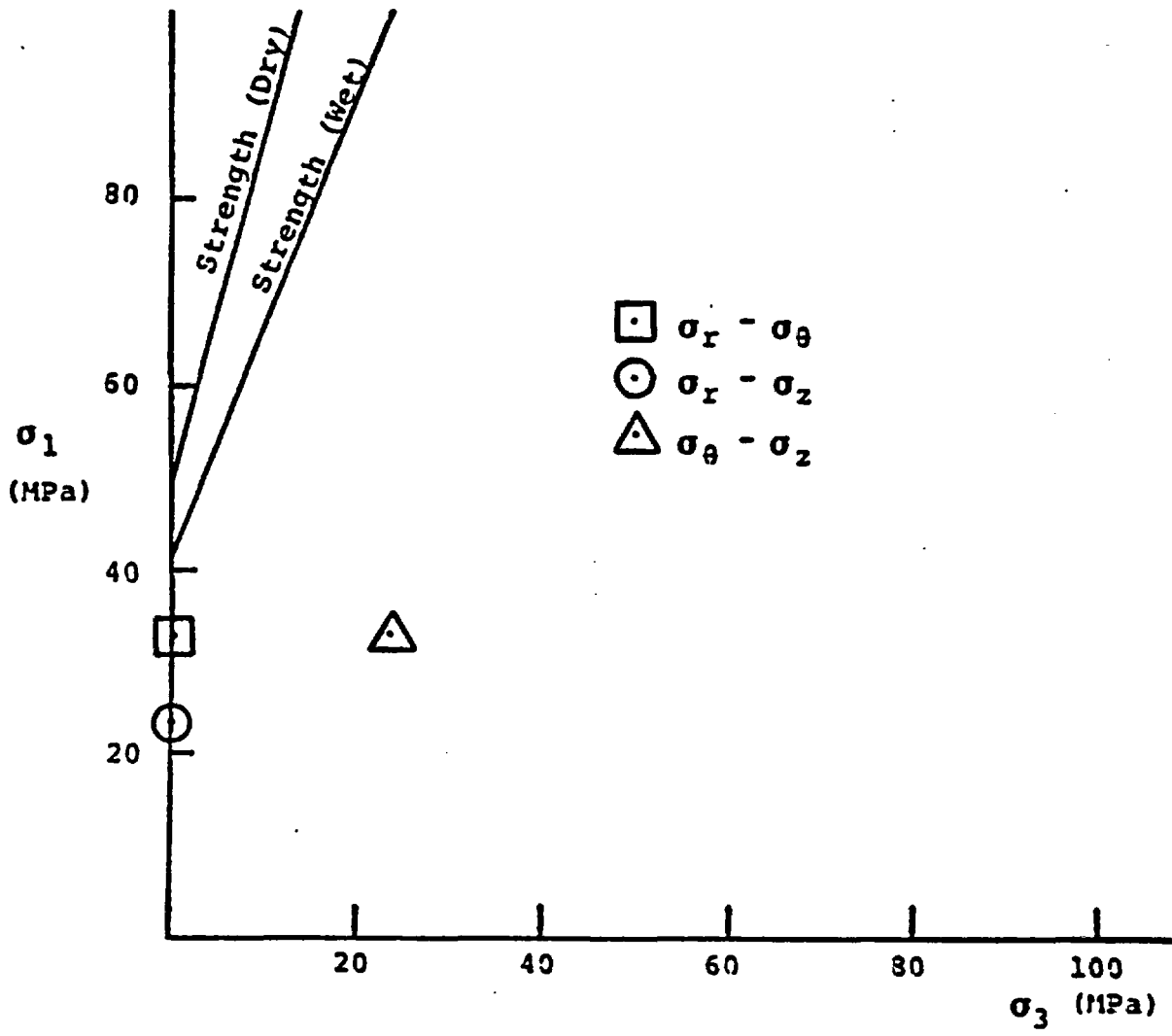


Figure 7. Stress-Strength Comparison for the Tram Layer

Therefore,

$$M_{\text{wet}} = \frac{24.11}{21.54} = 1.12$$

Dry Strength

$$S_{\text{Lab}} = 31.34 \text{ MPa}$$

so,

$$M_{\text{dry}} = \frac{31.34}{21.54} = 1.54$$

The M factors for the three formations are presented in Table 5. M cannot be less than one. The S_{RM} must be less than S_{Lab} presuming damage was not done to the lab samples during collection and preparation. If M is actually larger than the values presented in Table 5, then the rock mass strength at the boundary of the hole is less than the stress. This will produce rock failure. The strength reductions are expected to be of this order of magnitude or greater, and the development of a zone of failed rock around the shaft should be expected for Case 1.

TABLE 5

MAXIMUM VALUES OF M WITHOUT
SHAFT WALL FAILURE

<u>Formation</u>	<u>M Factors</u>	
	<u>Wet</u>	<u>Dry</u>
Tuffaceous Beds	1.12	1.45
Bullfrog	1.44	1.68
Tram	1.25	1.47

3.2 Elastic Zone Material Properties Equal Plastic Zone Material Properties

If the material properties in the plastic (p subscript) and elastic (e subscript) zones are the same, for the angle of internal friction,

$$\phi_e = \phi_p = \phi, \text{ and for cohesion,}$$

$$c_e = c_p = c$$

It is assumed that failure occurs in the $r - \theta$ plane for $K > 0.5$ and that the plastic-elastic boundary occurs at radius R ($R =$ extent of the relaxed zone) (Figure 8). This assumption is based on Langkopf's (1982) work, which shows that K ranges from 0.7 to 0.8. If failure occurs around the shaft, then as the distance away from the wall is increased there will be some radius (R) where the material is elastic again. The radial pressure applied to the rockwall is P_i . In the special case where the shaft is unlined, $P_i = 0$. In the plastic region, $a < r < R$, the stress equilibrium equation (Jaeger and Cook, 1969) is applied:

$$\frac{d\sigma_r}{dr} + \frac{\sigma_r - \sigma_\theta}{r} = 0 \quad (9)$$

The Mohr-Coulomb failure criterion (Equation 6) can be written as

$$\sigma_\theta = \sigma_0 + \sigma_r \tan \beta \quad (10)$$

where

$$\sigma_1 = \sigma_\theta \quad , \text{ and}$$

$$\sigma_3 = \sigma_r \quad .$$

Substitution of Equation 10 into Equation 9 yields

$$\frac{d\sigma_r}{dr} = \frac{\sigma_0 + (\tan \beta - 1) \sigma_r}{r} \quad .$$

Integrating and evaluating for boundary condition,

$$\sigma_r = P_i \quad \text{for } r = a,$$

yields

$$\sigma_r = \frac{\sigma_0}{1 - \tan \beta} + \left(P_i - \frac{\sigma_0}{1 - \tan \beta} \right) \left(\frac{r}{a} \right)^{(\tan \beta - 1)} \quad (11)$$

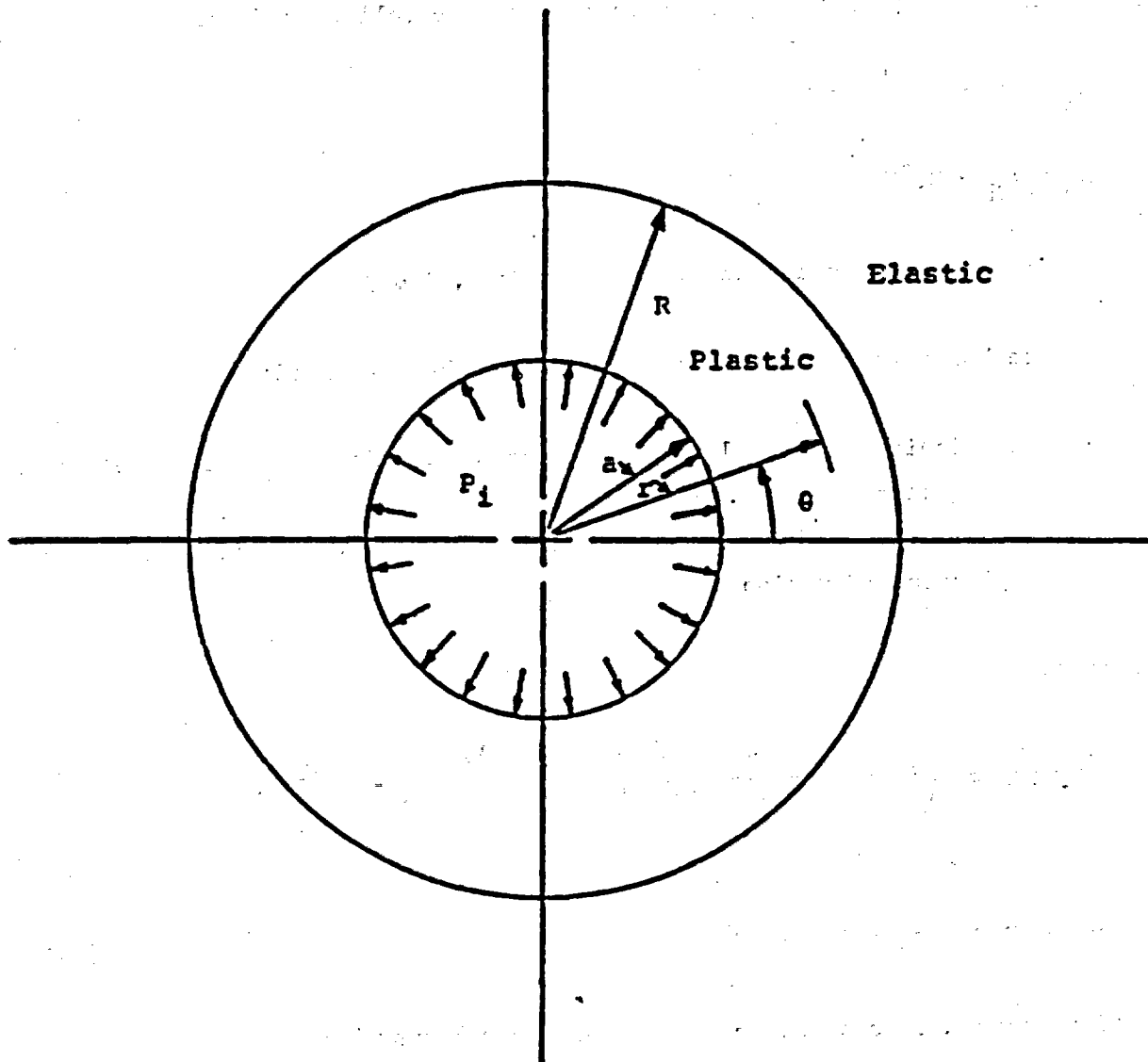


Figure 8. Diagrammatic Representation of the Plastic Zone Around a Shaft

Substitution of Equation 11 into Equation 10 yields

$$\sigma_{\theta} = \frac{\sigma_0}{1 - \tan \beta} + \tan \beta \left(P_i - \frac{\sigma_0}{1 - \tan \beta} \right) \left(\frac{r}{a} \right)^{(\tan \beta - 1)} \quad (12)$$

In the elastic region $r > R$, the solution has the following form:

$$\sigma_r = \sigma_H - Br^{-2}, \text{ and} \quad (13)$$

$$\sigma_{\theta} = \sigma_H + Br^{-2} \quad (14)$$

where B is an unknown constant (Jaeger and Cook, 1969).

At the boundary $r = R$, two conditions must be satisfied:

- continuity of radial stress requires that Equations 11 and 13 must be equal and
- the stresses given by Equations 13 and 14 must satisfy the Failure Criterion (Equation 10).

Therefore,

$$\frac{\sigma_0}{1 - \tan \beta} + \left(P_i - \frac{\sigma_0}{1 - \tan \beta} \right) \left(\frac{R}{a} \right)^{(\tan \beta - 1)} = \sigma_H - BR^{-2} \quad (15)$$

and

$$\sigma_H + BR^{-2} = \sigma_0 + (\sigma_H - BR^{-2}) \tan \beta \quad (16)$$

Equations 15 and 16 can now be solved for the unknowns B and R.

$$\frac{R}{a} = \left[\frac{2[\sigma_H(\tan \beta - 1) + \sigma_0]}{[P_i(\tan \beta - 1) + \sigma_0](\tan \beta + 1)} \right]^{\frac{1}{\tan \beta - 1}} \quad (17)$$

$$B = \frac{R^2[\sigma_H(\tan \beta - 1) + \sigma_0]}{\tan \beta + 1} \quad (18)$$

Equations 15, 17, and 18 are those originally derived by Westergaard (1907) and discussed by Terzaghi (1943). [Talobre (1957, 1967) has included incorrect versions of these equations in his books.]

If $\sigma_0 = 0$ (cohesionless material), Equations 11, 12, and 17 reduce to

$$\sigma_r = P_i \left(\frac{r}{a} \right)^{(\tan \beta - 1)},$$

$$\sigma_\theta = \tan \beta P_i \left(\frac{r}{a} \right), \text{ and}$$

$$\frac{R}{a} = \left[\frac{2\sigma_H}{P_i (\tan \beta + 1)} \right]^{\frac{1}{\tan \beta - 1}}, \text{ respectively.}$$

These equations were obtained by Fenner (1938), Terzaghi (1943), and Labasse (1949). Jaeger and Cook (1969) have shown that, in the region $a < r < R$, the slip line directions are inclined to that of the least compressive stress (the radial stress) by angle λ . As a result,

$$\frac{1}{r} \frac{dr}{d\theta} = \pm \cot \lambda.$$

The extent of the relaxed zone as a function of P_i can be determined by solving Equation 17 for P_i :

$$P_i = \left[\sigma_H - \frac{\sigma_H (\tan \beta - 1) + \sigma_0}{\tan \beta + 1} - \frac{\sigma_0}{1 - \tan \beta} \right] \left(\frac{a}{R} \right)^{(\tan \beta - 1)} + \frac{\sigma_0}{1 - \tan \beta}.$$

Simplifying,

$$P_i = \left[\frac{2\sigma_H}{\tan \beta + 1} - \frac{2\sigma_0}{(\tan \beta + 1)(1 - \tan \beta)} \right] \left(\frac{a}{R} \right)^{(\tan \beta - 1)} + \frac{\sigma_0}{1 - \tan \beta}$$

or

$$P_i = \frac{2}{\tan \beta + 1} \left(\sigma_H + \frac{\sigma_0}{\tan \beta - 1} \right) \left(\frac{a}{R} \right)^{(\tan \beta - 1)} - \frac{\sigma_0}{\tan \beta - 1}.$$

This is the form used by Terzaghi (1943).

3.3 Elastic Zone Material Properties Do Not Equal Plastic Zone Material Properties

The previous representation in which the cohesion and angle of internal friction are the same in both the elastic and plastic zones is not very realistic when considering a shaft in rock. The cohesion in particular would be expected to be quite different in the plastic and elastic zones. This problem has been discussed by Jaeger and Cook (1969) and Ladanyi (1974). The failure criterion of the rock in the elastic zone ($r > R$) becomes

$$\sigma_{\theta} = \sigma_0' + \sigma_r \tan \beta'$$

where

σ_0' = unconfined compressive strength of rock mass,

$$\tan \beta' = \frac{1 + \sin \phi'}{1 - \sin \phi'} \quad \text{and}$$

ϕ' = angle of internal friction for the rock mass.

The preceding analysis applies except that Equation 16 is replaced by

$$\sigma_H + BR^{-2} = \sigma_0' + (\sigma_H - BR^{-2}) \tan \beta' \quad (19)$$

Radial stress continuity at the elastic-plastic boundary means that on the plastic side

$$\sigma_H - BR^{-2} = \frac{\sigma_0}{1 - \tan \beta} + \left(P_1 - \frac{\sigma_0}{1 - \tan \beta} \right) \left(\frac{R}{a} \right)^{(\tan \beta - 1)} \quad (20)$$

Solving Equations 19 and 20 for R and B yields

$$\frac{R}{a} = \left[\frac{(2\sigma_H - \sigma_0') (1 - \tan \beta) - \sigma_0 (1 + \tan \beta')}{(1 + \tan \beta') [P_1 (1 - \tan \beta) - \sigma_0]} \right]^{\frac{1}{\tan \beta - 1}} \quad \text{and}$$

$$B = \frac{R^2 [\sigma_H (\tan \beta' - 1) + \sigma_0']}{1 + \tan \beta'}$$

These reduce to Equations 17 and 18 when

$$\sigma_0' = \sigma_0 \quad \text{and} \quad \beta' = \beta$$

From laboratory triaxial tests performed on broken and intact coal measures (strata containing coal beds, particularly those of the carboniferous) (Figure 9), Hobbs (1966) suggests that

$$\tan \beta \text{ (broken)} \cong \tan \beta' \text{ (intact)} .$$

If this is true, the major difference between the Terzaghi (1943) and Jaeger and Cook (1969) equations lies in the cohesion terms.

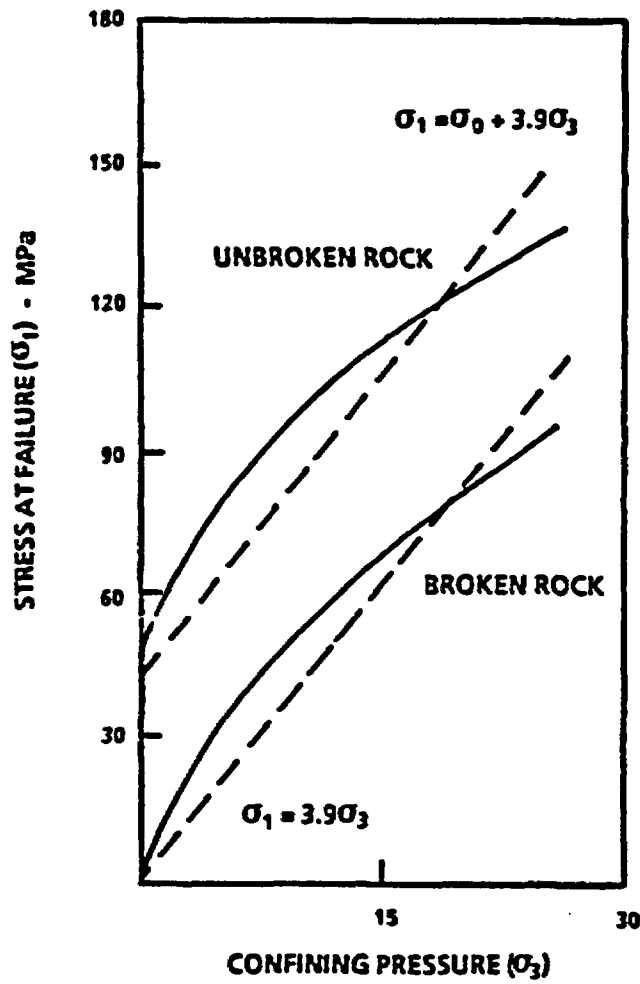


Figure 9. Relationship Between Confining Pressure and Stress at Failure for Silty Mudstone (Bilstorpe Colliery) (Wilson, 1972; Hobbs, 1966)

4.0 SHAFT LINING ANALYSIS

4.1 Introduction

Labasse (1949) has considered the design of shaft linings through horizons that are assumed to have zero cohesion. His approach is used here to illustrate the principles involved. His discussion of the failure process is quoted below.

When at the shaft wall, the rock does not resist adequately but fails, the shaft becomes surrounded with a ring of "relaxed ground"; i.e., separated from the mass, dislocated, fractured into large and small pieces which can slide upon and interlock with each other.

These pieces, by being dislodged, remove the constraint from a second ring of rock situated further into the rock mass. The latter (ring) is thus subjected to a greater principal stress difference (than before constraint removed) and in like manner fails also, when the extreme principal stresses become such that they give a Mohr's circle tangent to the intrinsic curve for the material. In relaxing, this second ring releases a third ring which likewise fractures, releases a fourth ring which in turn breaks, and so on.

Thus, slowly--since it proceeds by sliding where frictional forces are high--progressively, and in concentric zones, the shaft becomes surrounded by a region of relaxed ground. But upon releasing the pieces develop an apparent increase in rock volume which causes them to flow towards the opening, decreasing its cross section and exerting a thrust on the shaft lining. This thrust is developed as soon as the rock touches the lining and increases as the contact becomes more intimate.

If the support is sufficiently resistant, it develops an increasing "counterthrust" which ends by bringing the ground stresses into equilibrium and arresting the relaxation phenomena; a "state of equilibrium" is established.

When it (the support) cannot resist, it will deform if it is elastic, otherwise it will break and there will be a fall of ground.

The decrease in the intensity of the equilibrium thrust with the extension of relaxation into the rock mass may be explained by "arching" of the rocks: the broken pieces grip each other due to roughness and interlocking of surfaces in contact forming the two "lips" of the same fracture. As relaxation progresses, the new zones compress the regions closer to the shaft wall, increasing the arching effect in these regions creating a protective ring which reduces the pressure exerted on the support.

The stress equations in the broken zone ($a < r < R$) are

$$\sigma_r = P_i \left(\frac{r}{a} \right)^\alpha \quad \text{and} \quad (21)$$

$$\sigma_\theta = P_i \left(\frac{r}{a} \right)^\alpha \frac{1 + \sin \phi}{1 - \sin \phi}$$

where

$$\alpha = \frac{2 \sin \phi}{1 - \sin \phi} = \tan \beta - 1 \quad \text{and}$$

$$\frac{1 + \sin \phi}{1 - \sin \phi} = \tan \beta \quad (\text{Equation 7}) \quad .$$

In the elastic region ($r > R$), the stresses are given by

$$\sigma_r = \frac{(1 - R^2 \sin \phi)}{r^2} \sigma_H \quad \text{and}$$

$$\sigma_\theta = \frac{(1 + R^2 \sin \phi)}{r^2} \sigma_H \quad .$$

On the elastic side of the elastic-plastic boundary, these become

$$\sigma_r = (1 - \sin \phi) \sigma_H \quad \text{and} \quad (22)$$

$$\sigma_\theta = (1 + \sin \phi) \sigma_H \quad .$$

Stress continuity at the boundary can be calculated by combining Equations 21 and 22 as follows

$$P_i \left(\frac{R}{a} \right)^\alpha = (1 - \sin \phi) \sigma_H \quad .$$

As a result,

$$P_i = (1 - \sin \phi) \left(\frac{a}{R} \right)^\alpha \sigma_H \quad . \quad (23)$$

From Equation 23 the following conclusions can be drawn:

- If the lining were installed before initiation of relaxation ($R = a$), the support required of the lining if rock failure is to be prevented would be a maximum. The lining must be capable of resisting

$$P_i(\text{max}) = (1 - \sin \phi) \sigma_H$$

- With the development of a relaxed zone ($R > a$) before installation of the lining, the required lining support to achieve equilibrium is reduced.
- The lining pressure decreases with increasing coefficient of internal friction.

Labasse (1949) indicates

The required dimensions of a shaft lining depend naturally on the forces to which it is subjected. If the ground withstands the elastic stresses developed as a result of sinking then support is unnecessary since the ground will stand alone.

If the ground is relaxed, a lining becomes essential in order to prevent the fall of dislodged rock, to arrest dilatation of the latter, and finally to prevent any deformation of the shaft that cannot be tolerated because of hoisting installations.

The problem, therefore, is one of finding the value of the equilibrium thrust " P_i " and consequently the radius " a " as a function of time.

This function can only be determined from experience. The rate of development of relaxation varies not only with the nature of the ground and the intensity of the pressures but also on the type of support (and the method of excavation^a).

Labasse (1949) indicates the following relaxation rates at medium depths are appropriate:

- several millimeters/day for hard rock, and
- several centimeters/day for weak rock.

^a Added by the present author.

Accompanying the development of the relaxed zone is a "bulking" of the rock between $r = a$ and $r = R$. Bulking occurs in the process of fracturing when new surfaces are developed and the resulting particles do not fit as tightly together (there are voids between some previously mating surfaces), hence, the broken rock occupies a greater volume than the nonbroken rock. There is also a volume expansion of the elastic rock as the applied stresses are reduced (calculated using bulk modulus). The inelastic portion resulting from the development of new surfaces is larger in soft rocks and is investigated here.

Before relaxation, the area contained in the annulus, $a \leq r \leq R$, is

$$A_b = \pi (R^2 - a^2) .$$

After relaxation the area is

$$A_a = K_0 \pi (R^2 - a^2) ,$$

where

K_0 = expansion coefficient.

The value of K_0 is suggested by Labasse to be of the order of 1.1. ($K_0 = 1.1$ is probably conservatively large. However, there are no available data to predict K_0 accurately, therefore, Labasse's estimate of K_0 is adequate for this analysis). The shaft radius (X) after the development of the relaxed zone can be found using

$$R^2 - X^2 = K_0 (R^2 - a^2)$$

or

$$X = R \left[1 - K_0 \left(1 - \frac{a^2}{R^2} \right) \right]^{1/2} .$$

The inward radial plastic displacement (U_w) of the excavated shaft wall would be

$$U_w = a - X .$$

A rock stiffness (K_R) curve can be constructed using the pressure P_i and the corresponding U_w . This curve is then compared to the corresponding curve for the lining selected.

4.2 Example of Rock Stiffness Calculation

The development of the plastic zone can be obtained using

$$P_i = \sigma_H (1 - \sin \phi) \left(\frac{a}{R} \right)^\alpha$$

assuming

$$\begin{aligned} \sigma_H &= 15 \text{ MPa,} \\ \phi &= 30^\circ, \text{ and} \\ a &= 1.5 \text{ m.} \end{aligned}$$

The results are given in Table 6 and Figure 10.

TABLE 6

RADIAL DISPLACEMENT (U_w) OF THE SHAFT WALL
AS A FUNCTION OF APPLIED INNER PRESSURE (P_i)

<u>R(m)</u>	<u>a/R</u>	<u>P_i (MPa)</u>	<u>U_w (mm)</u>
1.50	1.00	7.54	0.0
1.52	0.99	7.30	2.0
1.54	0.97	7.12	4.1
1.56	0.96	6.93	6.1
1.60	0.94	6.59	10.4
1.70	0.88	5.84	21.5
1.80	0.83	5.21	33.4
1.90	0.79	4.67	46.0
2.00	0.75	4.22	59.5
2.50	0.60	2.71	139.9
3.00	0.50	1.88	245.0
3.50	0.43	1.39	382.0
4.00	0.38	1.05	565.0

It will be assumed that the lining can be represented by a thick-walled pipe as shown in Figure 11, where

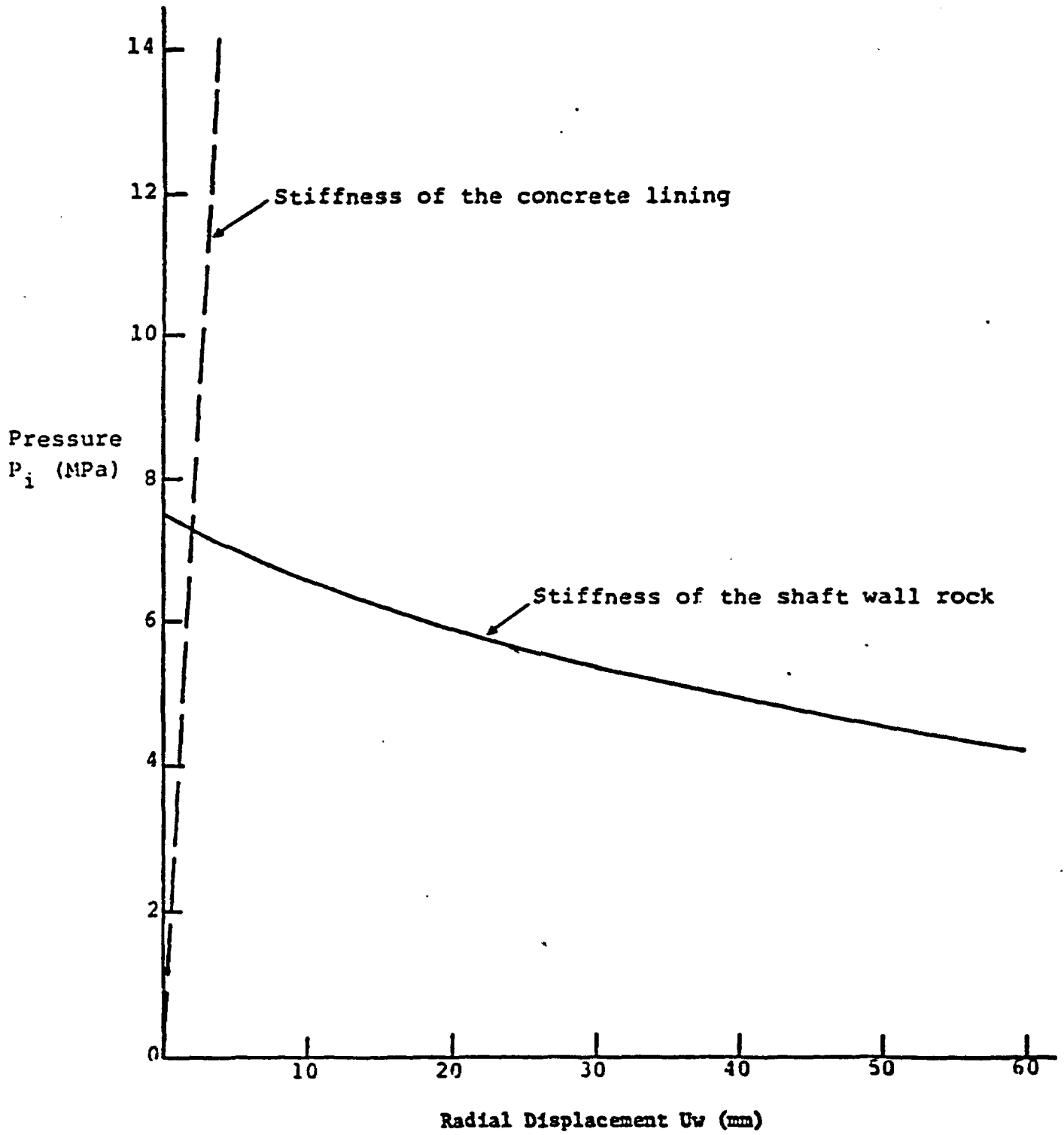


Figure 10. Lining Pressure--Radial Wall Displacement (for Equilibrium) for the Example Problem

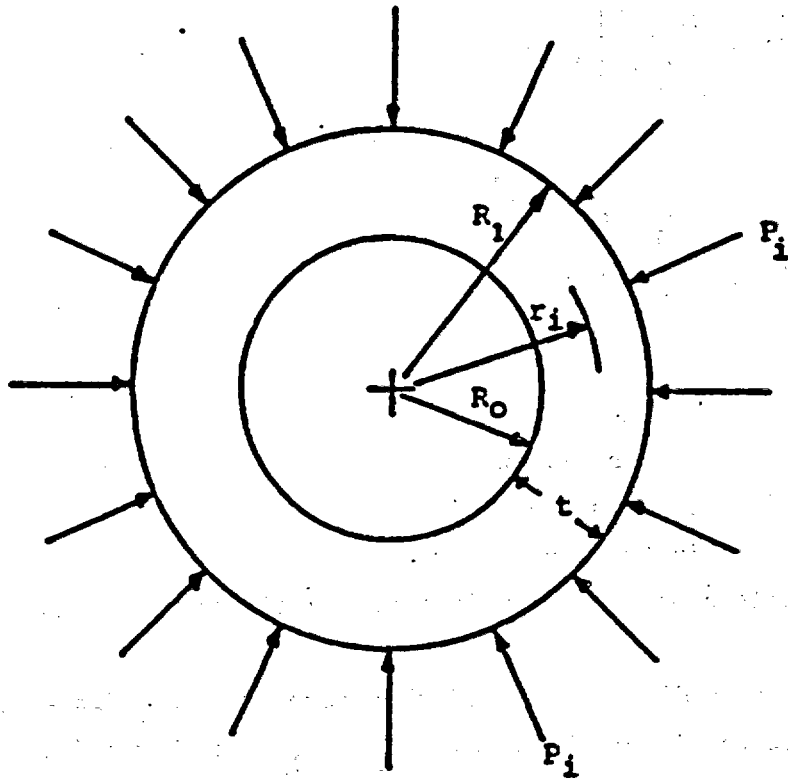


Figure 11. Diagrammatic Representation of the Shaft Lining

R_0 = inner radius of the lining,
 R_1 = outer radius of the lining,
 $t = R_1 - R_0$ = lining thickness,
 r_i = radius to an intermediate point, and
 P_i = pressure applied to the lining.

The stresses arising in the lining due to the weight of the concrete are

$$\sigma_z' = \gamma'H \quad ,$$

$$\sigma_r' = \frac{P_i R_1^2}{R_1^2 - R_0^2} \left[1 - \left(\frac{R_0}{r_i} \right)^2 \right] \quad , \text{ and}$$

$$\sigma_\theta' = P_i \frac{R_1^2}{R_1^2 - R_0^2} \left[1 + \left(\frac{R_0}{r_i} \right)^2 \right] \quad .$$

where

σ_r' = radial stress in the lining,
 σ_θ' = tangential stress in the lining,
 σ_z' = axial stress in the lining, and
 γ' = stress/unit depth due to weight of the lining material.

The maximum stress difference (and therefore the most dangerous stress condition) occurs at the inner shaft wall, $r_i = R_0$. At this point

$$\sigma_r' = 0 \quad ,$$

$$\sigma_\theta' = \frac{2 P_i R_1^2}{R_1^2 - R_0^2} \quad , \text{ and} \quad (24)$$

$$\sigma_z' = \gamma'H \quad .$$

It is assumed that any lining failure is the result of stresses σ_r and σ_θ . If the lining is constructed of concrete having a designed compressive strength of f_c' , the safety factor becomes

$$FS = \frac{\text{Strength}}{\text{Stress}} = \frac{f_c'}{\sigma_\theta} \quad (25)$$

Substituting Equation 24 into 25 yields

$$FS = \frac{f_c'}{2P_i \left(\frac{R_1^2}{R_1^2 - R_0^2} \right)} = \frac{f_c'}{2P_i} \left(1 - \frac{R_0^2}{R_1^2} \right)$$

Since $R_1 = R_0 + t$,

$$FS = \frac{f_c'}{2P_i} \left[1 - \frac{R_0^2}{(R_0 + t)^2} \right] = \frac{f_c'}{2P_i} \left[1 - \frac{1}{\left(1 + \frac{t}{R_0} \right)^2} \right]$$

The relationship between the stress on the outside of the lining (P_i) and the radial displacement (U_r) of the outer wall is given approximately by

$$P_i = \frac{E_b t}{R_1^2} (U_r),$$

where

E_b = modulus of elasticity of the lining, and
 R_1 = outer radius of the support on installation.

4.3 Example of Lining Stiffness Calculation

It is assumed that the lining is constructed of concrete. Therefore,

$$R_1 = 1.5 \text{ m,}$$

$$R_0 = 1.2 \text{ m,}$$

$$t = 1.5 - 1.2 = 0.3 \text{ m,}$$

$$f_c' = \text{compressive strength of concrete (MPa)} \\ = 35 \text{ MPa, and}$$

$$E_b = 4,730 \sqrt{f_c'} = \text{Young's modulus of concrete (MPa)}$$

$$= 28,000 \text{ MPa.}$$

Thus, the radial pressure that would produce lining failure is (Equations 24 and 25, with FS = 1.5)

$$P_i(\text{max}) = \frac{f_c' (1.5^2 - 1.2^2)}{1.5^2} = 12.60 \text{ MPa}$$

The stiffness for the lining would be

$$K_L = \frac{P_i}{U_r} = \frac{28,000(0.30)}{1.5^2} = 3,733 \text{ MPa/m.}$$

Values of the stress (P_i) and displacement (U_r) are given in Table 7. The maximum radial displacement that the shaft can undergo before failure is 3.38 mm. This stiffness curve has been superimposed on Figure 10. The equilibrium pressure is about 7.3 MPa.

TABLE 7

RADIAL DISPLACEMENT (U_r) OF THE OUTER
LINING WALL AS A FUNCTION OF PRESSURE (P_i)

Pressure (P_i) (MPa)	Radial Displacement (U_r) (mm)
3.73	1.0
5.60	1.5
7.47	2.0
9.33	2.5
11.20	3.0
12.60 ^a	3.4
14.93	4.0
18.67	5.0

^a Pressure at which lining failure occurs.

4.4 Lining Selection for the Generic Tuff Shaft

The basic equations required for a conservative lining design are given above. Here they are applied to the generic tuff formations. The following assumptions are made:

- Shaft bored, diameter = 3 m
- Shaft lining:

$$R_0 = 1.2 \text{ m}$$

$$R_1 = 1.5 \text{ m}$$

$$f_c' = 35 \text{ MPa}$$

$$E_b = 28,000 \text{ MPa}$$

$$t = 0.3 \text{ m}$$

$$FS = 1.5$$

- Rock:

Cohesionless, $c = 0$

Angle of internal friction = lab value, and

- Shaft lining installed after elastic relief but before development of a plastic zone.

The maximum tangential stress (σ_θ'), which can safely be taken by the lining, is (assuming a safety factor of 1.5)

$$\sigma_\theta' = \frac{f_c'}{1.5} = \frac{35}{1.5} = 23.33 \text{ MPa}$$

The required pressure to prevent relaxation around the shaft is calculated using

$$P_i \text{ (required)} = \sigma_H (1 - \sin \phi)$$

The values used for the calculations and the resulting required pressures are given in Table 8.

TABLE 8
PRESSURE REQUIRED TO PREVENT THE FORMATION
OF A RELAXED ZONE AROUND THE SHAFT

Formation	Horizontal Field Stress (σ_H) (MPa)	Laboratory Compressive Strength (MPa)		Friction Angle (Degrees)		P_i (required) (MPa)	
		Wet	Dry	Wet	Dry	Wet	Dry
Tuffaceous Beds	10.77	24.1	31.3	11	25	8.71	6.22
Bullfrog	14.58	41.9	41.9	25	35	8.42	6.22
Tram	16.71	41.9	41.9	25	35	9.65	7.13

The allowable external pressure on the shaft (P_i allowable) would be

$$P_i \text{ (allowable)} = \sigma_{\theta} \left(\frac{R_1^2 - R_0^2}{2 R_1^2} \right) = 4.20 \text{ MPa .}$$

This suggests that, for the no-cohesion case and a safety factor of 1.5, a 0.3-m-thick shaft wall would not be able to support the rock. Such a lining would have to be installed leaving a gap between the lining and the wall to allow for relaxation.

If the lining had a thickness of 0.60 m,

$$R_1 = 1.5 \text{ m}$$

and

$$R_0 = 0.9 \text{ m.}$$

For this case,

$$P_i \text{ (allowable)} = 7.46 \text{ MPa.}$$

This value (compared with those in Table 8) yields a safety factor greater than 1.5 under dry conditions. For wet conditions, the safety factor would vary from 1.16 to 1.33.

If the cohesion is included, the thickness of the required lining is reduced considerably. It is assumed that

$$\phi' = \phi = \phi_{\text{laboratory}}$$

and

$$\sigma_0' , \sigma_0 = \frac{\sigma_{\text{laboratory}}}{M}$$

Here, M is the strength reduction factor, and values of 1, 2, 3, 4, and 5 are applied.

The equation to be used is

$$P_i \text{ (required)} = \frac{2}{\tan \beta + 1} \left(\sigma_H + \frac{\sigma_0}{\tan \beta - 1} \right) \left(\frac{a}{R} \right) (\tan \beta - 1) - \frac{\sigma_0}{\tan \beta - 1}$$

For $R = a$, it becomes

$$P_i \text{ (required)} = P_i \text{ (no cohesion)} - \Delta P$$

where

$$\Delta P = \frac{\sigma_0 (1 - \sin \phi)}{2}$$

Use of the appropriate unconfined compressive strengths and angles of internal friction for the three formations yields the values for ΔP in Table 9 and P_i (required) in Table 10.

TABLE 9

CONTRIBUTION OF COHESION (ΔP) IN PREVENTING
DEVELOPMENT OF A RELAXED ZONE AROUND THE SHAFT

<u>Formation</u>	<u>Condition</u>	<u>ΔP (MPa)</u>				
		<u>Laboratory Strength Reduction Factors</u>				
		<u>M=1</u>	<u>M=2</u>	<u>M=3</u>	<u>M=4</u>	<u>M=5</u>
Tuffaceous	Wet	9.75	4.88	3.25	2.44	1.95
	Dry	9.04	4.52	3.01	2.26	1.81
Bullfrog	Wet	12.10	6.05	4.03	3.02	2.42
	Dry	10.46	5.23	3.49	2.62	2.09
Tram	Wet	12.10	6.05	4.03	3.02	2.42
	Dry	10.46	5.23	3.49	2.62	2.09

TABLE 10

SHAFT LINING PRESSURES DEVELOPED IN
COHESIVE FORMATIONS

<u>Formation</u>	<u>Condition</u>	<u>P_i (required) (MPa)</u>				
		<u>Strength Reduction Factors</u>				
		<u>M=1</u>	<u>M=2</u>	<u>M=3</u>	<u>M=4</u>	<u>M=5</u>
Tuffaceous	Wet	0	3.83	5.46	6.27	6.76
	Dry	0	1.70	3.21	3.96	4.41
Bullfrog	Wet	0	2.37	4.39	5.40	6.00
	Dry	0	0.99	2.73	3.60	4.13
Tram	Wet	0	3.60	5.62	6.63	7.23
	Dry	0	1.90	3.64	4.51	5.04

The shaded values in Table 10 correspond to values of P_i (required) greater than P_i (allowable) for a 0.3-m-thick lining. The in situ strength is extremely important to lining design, particularly if the material is wet. Under dry conditions, the safety factor would range from 6.67 to 1.31 for the

entire range of M values. In all probability, a 0.3-m-thick concrete lining would suffice. The same is not true for wet rock conditions with M values of 4 to 5. Here a thicker shaft would be required. It would be useful (and not difficult) to generate a set of liner thicknesses as a function of shaft diameter that are required to prevent failure under conditions described in Table 10.

The required lining thickness (assuming a safety factor of 1.5) to prevent the development of a broken zone in cohesive formations is summarized in Table 11. As can be seen, a lining thickness of 0.3 m would be sufficient for strength reduction factors of about 3 assuming dry rock properties apply. For wet rock properties, a lining thickness of 0.4 m would be sufficient for a strength reduction factor up to 2. For higher strength reduction factors, much greater lining thicknesses would be required. In practice, some relaxation of the rock around the shaft would occur before lining and the required pressure would be less than that presented in Table 10.

TABLE 11
 REQUIRED SHAFT LINING THICKNESS
 IN COHESIVE FORMATIONS
 (Safety Factor of 1.5)

<u>Formation</u>	<u>Condition</u>	<u>Lining Thickness (m)</u>				
		<u>Strength Reduction Factors</u>				
		<u>M=1</u>	<u>M=2</u>	<u>M=3</u>	<u>M=4</u>	<u>M=5</u>
Tuffaceous	Wet	0	0.41	1.40	2.10	2.63
	Dry	0	0.00	0.12	0.47	0.72
Bullfrog	Wet	0	0.00	0.70	1.35	1.84
	Dry	0	0.00	0.00	0.30	0.56
Tram	Wet	0	0.30	1.52	2.48	3.24
	Dry	0	0.00	0.32	0.77	1.10

5.0 ANALYSIS OF THE DATA FROM THE MT. TAYLOR SHAFT

Abel et al. (1979) recently published a paper dealing with an evaluation of the concrete lining design for the Mt. Taylor shaft (Gulf Minerals, Grants, New Mexico). The shaft was sunk to a depth of about 1,006 m through Mancos Shale and Westwater Sandstones using conventional drill and blasting shaft-sinking techniques. The inside diameter of the concrete lining was 4.3 m with a nominal wall thickness of 0.6 m. The results of laboratory strength tests conducted on samples of the rock are given in Figures 12 and 13. The laboratory strengths were reduced to take into account rock mass properties. The values used in the analysis are given in Table 12.

TABLE 12
VALUES USED FOR THE MT. TAYLOR SHAFT ANALYSIS^a

<u>Depth (m)</u>	<u>Rock Type</u>	<u>Horizontal Field Stress (MPa)</u>	<u>Angle of Internal Friction ϕ</u>	<u>Rock Mass Compressive Strength (MPa)</u>
286.5	Mancos Shale	4.6	32.1°	6.9
618.7	Mancos Shale	9.9	32.1°	6.9
924.2	Westwater Sandstone	14.8	29.2°	3.5

^a Data from Abel et al., 1979.

^b Reduced by factor of 7 from laboratory value.

^c Reduced by factor of 5 from laboratory value.

The expected lining pressures can be calculated using the theory presented in earlier sections. For the case of no cohesion and no relaxation zone development,

$$P_i = \sigma_H (1 - \sin \phi)$$

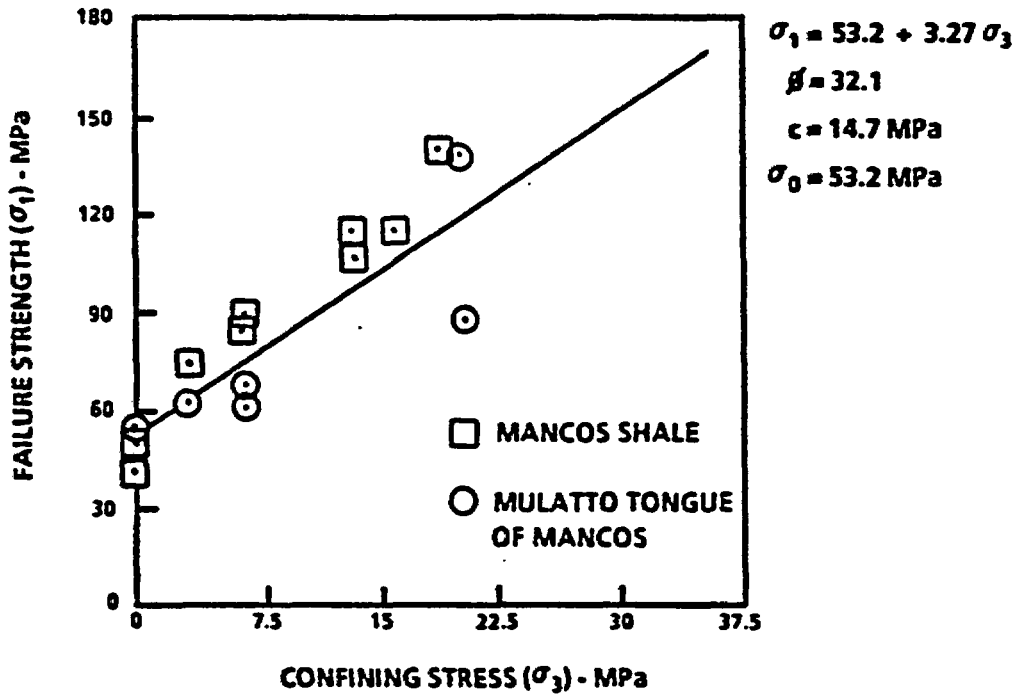


Figure 12. Triaxial Compression Test Results, Mancos Shale Formation (Abel et al., 1979)

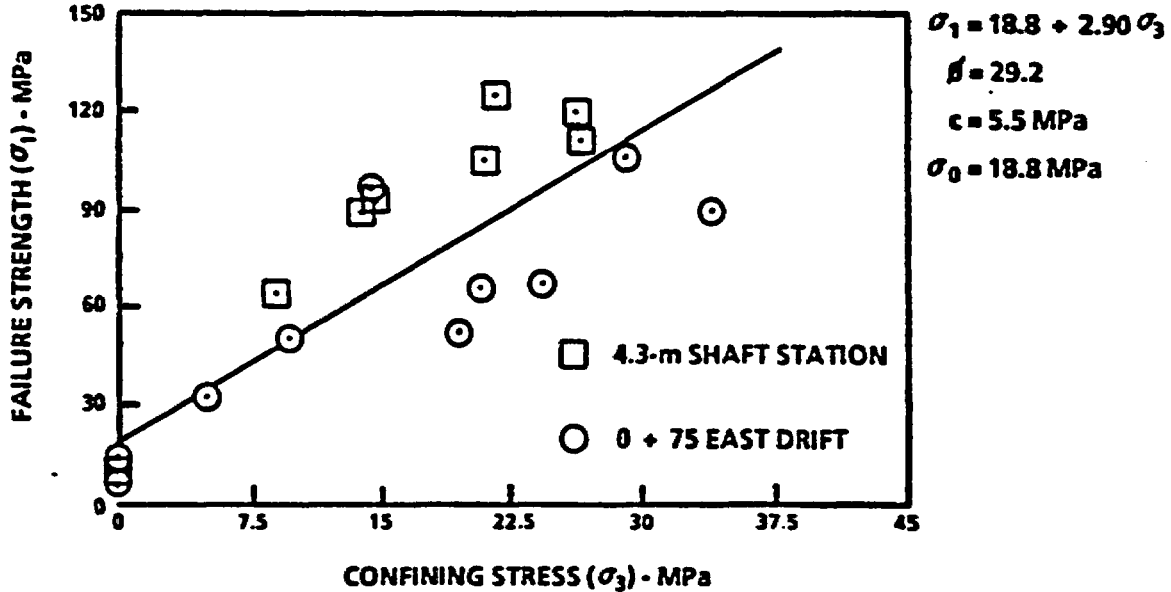


Figure 13. Triaxial Compression Test Results, Upper Westwater Canyon Member of the Morrison Formation (Abel et al., 1979)

With cohesion the formula is

$$P_i = \sigma_H (1 - \sin \phi) - \sigma_0 \frac{(1 - \sin \phi)}{2}$$

For these two conditions, the maximum expected lining pressures are given in Table 13.

TABLE 13
MEASURED AND EXPECTED LINING PRESSURES (P_i)

Depth (m)	Expected Lining Pressures (MPa)		Measured Lining Pressures (MPa)
	No Cohesion	Cohesion	
286.5	2.16	0.54	0.65
618.7	4.65	3.03	1.54
924.2	7.59	6.71	2.89

To monitor the lining pressure, Carlson strain cells were placed in the concrete lining at depths of 286.5, 618.7, and 924.2 m. The strain readings were converted into stresses and then into lining pressures, P_i . The average Carlson-based lining pressures are also given in Table 13. The measured pressures are considerably less than the predicted (based upon no relaxed zone).

With no broken zone development before shaft lining installation, the maximum shaft lining stresses would be predicted as given in Table 14.

TABLE 14
MAXIMUM SHAFT LINING STRESSES

Depth (m)	Maximum Lining Stress (MPa)	
	No Cohesion	Cohesion
286.5	10.93	2.72
618.7	23.56	15.36
924.2	38.43	30.26

At a depth of 924.2 m the shaft lining stresses, assuming no broken zone and no cohesion, exceed the assumed strength of the concrete (34.47 MPa).

If theory does hold, there must be a relaxed zone surrounding the shaft. The thickness of the relaxed zone is calculated assuming that the measured lining pressures reflect the equilibrium pressures according to equations derived by Terzaghi (1943).

No Cohesion

$$P_i = \sigma_H (1 - \sin \phi) \left(\frac{a}{R}\right)^\alpha$$

Cohesion

$$P_i = \sigma_H (1 - \sin \phi) \left(\frac{a}{R}\right)^\alpha - \left(\frac{\sigma_0 (1 - \sin \phi)}{2 \sin \phi}\right) 1 - (1 - \sin \phi) \left(\frac{a}{R}\right)^\alpha$$

The results are given in Table 15.

TABLE 15

PREDICTED RADIUS AND THICKNESS OF THE RELAXED ZONE (R) SURROUNDING THE SHAFT

Depth (m)	Relaxed Zone Radius (m)		Relaxed Zone Thickness (m)	
	No Cohesion	Cohesion	No Cohesion ^a	Cohesion
286.5	4.66	2.74	1.92	0.00
618.7	4.46	3.10	1.72	0.36
924.2	4.56	3.75	1.81	1.00

^a These values seem to be independent of depth.

This degree of relaxation could not occur after emplacement of the lining due to the bulking requirements. For example, the development of the relaxed zone for the case with cohesion is given in Table 16.

To accommodate these radial displacements after lining emplacement, the lining stresses would be those given in Table 17.

TABLE 16

ROCK WALL MOVEMENT REQUIRED TO ACHIEVE THE
OBSERVED LINING PRESSURE THROUGH BULKING

<u>Depth (m)</u>	<u>Shaft Radius (m)</u>		<u>Movement (m)</u>
	<u>Initial</u>	<u>Final</u>	
286.5	2.74	2.74	0.00
618.7	2.74	2.70	0.04
924.2	2.74	2.62	0.12

TABLE 17

MAXIMUM LINING STRESSES AS A RESULT
OF FULL BULKING OF THE RELAXED ZONE

<u>Depth (m)</u>	<u>Maximum Lining Stress (MPa)</u>
618.7	4.52×10^2
924.2	1.39×10^3

These values obviously are far in excess of the compressive strength of the concrete ($\cong 34.47$ MPa). The amount of additional radial displacement of the rock surrounding the shaft required to produce the measured lining pressures (through bulking) is given in Table 18. These small displacements could easily occur after shaft lining installation.

From the Mt. Taylor Shaft data, it is surmised that a blast-damage zone exists around the shaft and that the lining holds the pieces in place. Any further deterioration of the rock surrounding the shaft produces a slight compaction of the broken (relaxed) zone and some additional bulking. This is responsible for the lining pressures noted.

TABLE 18

RADIAL DISPLACEMENT (U)
OF THE OUTER SHAFT WALL NEEDED TO PRODUCE
THE OBSERVED PRESSURES

<u>Depth (m)</u>	<u>Pressure (MPa)</u>	<u>Radial Displacement (cm)</u>
286.5	0.65	0.028
618.7	1.54	0.068
924.2	2.89	0.130

6.0 CONCLUSIONS

The following conclusions are drawn based upon the specific assumptions considered in this report.

- The development of a stress-induced failure zone around a drilled, vertical, circular shaft depends upon the rock mass strength and the in situ stress field. For the Mohr-Coulomb yield criteria used, the rock mass strength can be expressed in terms of cohesion (c) and angle of internal friction (ϕ), or unconfined compressive strength (σ_0) and the passive pressure coefficient ($\tan \beta$).
- If the horizontal field stress is greater than one-half of the vertical field stress, failure (if it would occur) would be in the horizontal plane (radial and tangential stresses involved). Failure initiation is at the shaft wall.
- If the horizontal field stress is less than one-half of the vertical field stress, failure (if it would occur) would be in the vertical plane (radial and vertical stresses involved) at the shaft wall.
- The extent of any stress-induced failure zone around the shaft depends upon the magnitude of the field stresses, the rock mass strength, and the restraint provided by the lining.
- Since rock mass strength generally is inversely proportional to the volume of rock involved raised to some power, the extent of the broken zone would be expected to increase with shaft diameter (assuming the same stress field).
- The thickness of lining required depends upon the strength of the lining material, the safety factor used, the relative stiffness of the rock and support systems, the rock mass strength, the field stresses, the extent of the broken zone at the time of lining installation, and the shaft diameter.

- For the particular stress field and laboratory rock properties used in this report to illustrate the application of formulas,
 - No stress-induced failure zone would be expected to develop if the rock mass strength is equal to the laboratory-determined strength ($M = 1$).
 - A failure zone would occur if M is greater than the values given in Table 1.
- If the generic shaft were conventionally (drill and blast) sunk, as opposed to being drilled, a broken zone would be created during the excavation process. The relaxed zone development and resulting lining pressures could be considerably different and potentially much lower from a bored (drilled) shaft of the same basic diameter.
- The shape and extent of the failure zone, as well as lining requirements, would be different from those discussed in the report if the principal horizontal stresses were quite different. (In the analysis they have been assumed to be equal.)
- Considerable differences exist between theoretical analysis and actual field measurements. In the comparison summarized in this report, the theoretical analyses appear exceptionally conservative.

7.0 RECOMMENDATIONS

- It is quite likely that the actual M values are higher than those given in Table 5, and the presence of a failed zone should be considered in any shaft design calculation.
- Because both the type [vertical (r - z) or horizontal (r - θ plane)] and extent of the potential failure zone around a shaft are so dependent upon the field stresses and the rock mass strength, high priority should be placed upon obtaining the best possible estimates of these values.
- Little information exists regarding the rate of development of a relaxed (failed) zone. Such information would be important when evaluating lining installation alternatives.

8.0 REFERENCES

- Abel, J. A., Jr., J. E. Dowis, and D. P. Richards, "Concrete Shaft Lining Design," 20th U.S. Symposium on Rock Mechanics, Austin, Texas, 1979.
- Fenner, R., "Untersuchungen Zur Erkenntnis de Gebirgsdrucks," Gluckauf, August 13 and 20, 1938, pp 690-695.
- Hobbs, D. W., "A Study of the Behavior of a Broken Rock Under Triaxial Compression and Its Application to Mine Roadways," International Journal of Rock Mechanics and Mining Sciences, V. 3, 1966.
- Jaeger, J. C. and N. G. W. Cook, Fundamentals of Rock Mechanics, Methuen, London, 1969, pp 395-399.
- Labasse, J., "Ground Pressures in Coal Mines: II. Rock Pressures Around Shaft," Revue Universelle des Mines, V. 5, March 1949, pp 78-88 (translated from French by C. Fairhurst).
- Ladanyi, B. J., "Use of the Long-Term Strength Concept in Determination of Ground Pressure on Tunnel Linings," Third International Congress on Rock Mechanics, Denver, Colorado, 1974, IIB, pp 1150-1156.
- Langkopf, B. S., "Suggested Bounds for In Situ Stress Ratios For Use in Yucca Mountain Unit Selection Calculations," Memo of March 26, 1982, Sandia National Laboratories.
- Lappin, A. R., "Average Thermal and Mechanical Properties of the Tuffaceous Beds; and the Welded, Devitrified Tram and Bullfrog," Memo of April 5, 1982 to R. R. Peters, Sandia National Laboratories.
- Talobre, J. A., La Mecanique des Roches, Dunod, Paris, First Edition, 1957, pp 228-233.
- Talobre, J. A., La Mecanique des Roches, Dunod, Paris, Second Edition, 1967, pp 303-308.
- Terzaghi, K., Theoretical Soil Mechanics, Wiley, New York, 1943, pp 202-206.
- Westergaard, H. M., "Plastic State of Stress Around a Deep Well," J. Boston Soc. Civil Engrs., V. 27, 1907, pp 1-5.
- Wilson, A. H., "Research Into the Determination of Pillar Size, Part I: A Hypothesis Concerning Pillar Stability," The Mining Engineer, V. 131, no. 141, 1972, pp 409-417.

DISTRIBUTION LIST

B. C. Rusche (RW-1)
Director
Office of Civilian Radioactive
Waste Management
U.S. Department of Energy
Forrestal Building
Washington, DC 20585

J. W. Bennett (RW-20)
Office of Geologic Repositories
U.S. Department of Energy
Forrestal Building
Washington, DC 20585

Ralph Stein (RW-23)
Office of Geologic Repositories
U.S. Department of Energy
Forrestal Building
Washington, DC 20585

J. J. Fiore, (RW-22)
Program Management Division
Office of Geologic Repositories
U.S. Department of Energy
Forrestal Building
Washington, DC 20585

H. W. Frei (RW-23)
Engineering & Licensing Division
Office of Geologic Repositories
U.S. Department of Energy
Forrestal Building
Washington, DC 20585

E. S. Burton (RW-25)
Siting Division
Office of Geologic Repositories
U.S. Department of Energy
Forrestal Building
Washington, D.C. 20585

C. R. Cooley (RW-24)
Geosciences & Technology Division
Office of Geologic Repositories
U.S. Department of Energy
Forrestal Building
Washington, DC 20585

T. P. Longo (RW-25)
Program Management Division
Office of Geologic Repositories
U.S. Department of Energy
Forrestal Building
Washington, DC 20585

Cy Klingsberg (RW-24)
Geosciences and Technology Division
Office of Geologic Repositories
U. S. Department of Energy
Forrestal Building
Washington, DC 20585

B. G. Gale (RW-25)
Siting Division
Office of Geologic Repositories
U.S. Department of Energy
Forrestal Building
Washington, D.C. 20585

R. J. Blaney (RW-22)
Program Management Division
Office of Geologic Repositories
U.S. Department of Energy
Forrestal Building
Washington, DC 20585

R. W. Gale (RW-44)
Office of Policy, Integration, and
Outreach
U.S. Department of Energy
Forrestal Building
Washington, D.C. 20585

J. E. Shaheen (RW-44)
Outreach Programs
Office of Policy, Integration and
Outreach
U.S. Department of Energy
Forrestal Building
Washington, DC 20585

J. O. Neff
Salt Repository Project Office
U.S. Department of Energy
505 King Avenue
Columbus, OH 43201

D. C. Newton (EW-23)
Engineering & Licensing Division
Office of Geologic Repositories
U.S. Department of Energy
Forrestal Building
Washington, DC 20585

O. L. Olson, Manager
Basalt Waste Isolation Project Office
U.S. Department of Energy
Richland Operations Office
Post Office Box 550
Richland, WA 99352

D. L. Vieth, Director (4)
Waste Management Project Office
U.S. Department of Energy
Post Office Box 14100
Las Vegas, NV 89114

D. F. Miller, Director
Office of Public Affairs
U.S. Department of Energy
Post Office Box 14100
Las Vegas, NV 89114

D. A. Nowack (14)
Office of Public Affairs
U.S. Department of Energy
Post Office Box 14100
Las Vegas, NV 89114

B. W. Church, Director
Health Physics Division
U.S. Department of Energy
Post Office Box 14100
Las Vegas, NV 89114

Chief, Repository Projects Branch
Division of Waste Management
U.S. Nuclear Regulatory Commission
Washington, D.C. 20555

S. A. Mann, Manager
Crystalline Rock Project Office
U.S. Department of Energy
9800 South Cass Avenue
Argonne, IL 60439

K. Street, Jr.
Lawrence Livermore National
Laboratory
Post Office Box 808
Mail Stop L-209
Livermore, CA 94550

L. D. Ramspott (3)
Technical Project Officer for NNWSI
Lawrence Livermore National
Laboratory
P.O. Box 808
Mail Stop L-204
Livermore, CA 94550

J. E. Boudreau
Los Alamos National Laboratory
P.O. Box 1663
Mail Stop F-671
Los Alamos, NH 87545

D. T. Oakley (3)
Technical Project Officer for NNWSI
Los Alamos National Laboratory
P.O. Box 1663
Mail Stop F-671
Los Alamos, NH 87545

W. W. Dudley, Jr. (3)
Technical Project Officer for NNWSI
U.S. Geological Survey
Post Office Box 25046
418 Federal Center
Denver, CO 80225

NTS Section Leader
Repository Project Branch
Division of Waste Management
U.S. Nuclear Regulatory Commission
Washington, D.C. 20555

Document Control Center
Division of Waste Management
U.S. Nuclear Regulatory Commission
Washington, D.C. 20555

P. T. Prestholt
NRC Site Representative
1050 East Flamingo Road
Suite 319
Las Vegas, NV 89109

M. E. Spaeth
Technical Project Officer for NNWSI
Science Applications
International, Corp.
2769 South Highland Drive
Las Vegas, NV 89109

SAIC-T&MSS Library (2)
Science Applications
International, Corp.
2950 South Highland Drive
Las Vegas, NV 89109

W. S. Twenhofel, Consultant
Science Applications
International, Corp.
820 Estes Street
Lakewood, CO 80215

A. E. Gurrola
General Manager
Energy Support Division
Holmes & Narver, Inc.
Post Office Box 14340
Las Vegas, NV 89114

J. A. Cross, Manager
Las Vegas Branch
Yenix & Scisson, Inc.
Post Office Box 15408
Las Vegas, NV 89114

N. E. Carter
Battelle Columbus Laboratory
Office of Nuclear Waste Isolation
505 King Avenue
Columbus, OH 43201

V. M. Glanzman
U.S. Geological Survey
Post Office Box 25046
913 Federal Center
Denver, CO 80225

J. B. Wright
Technical Project Officer for NNWSI
Westinghouse Electric Corporation
Waste Technology Services Division
Nevada Operations
Post Office Box 708
Mail Stop 703
Mercury, NV 89023

ONWI Library (2)
Battelle Columbus Laboratory
Office of Nuclear Waste Isolation
505 King Avenue
Columbus, OH 43201

W. M. Hewitt, Program Manager
Roy F. Weston, Inc.
2301 Research Blvd., 3rd Floor
Rockville, MD 20850

H. D. Cunningham
General Manager
Reynolds Electrical &
Engineering Co., Inc.
Post Office Box 14400
Mail Stop 555
Las Vegas, NV 89114

T. Hay, Executive Assistant
Office of the Governor
State of Nevada
Capitol Complex
Carson City, NV 89710

R. R. Loux, Jr., Director (8)
Nuclear Waste Project Office
State of Nevada
Capitol Complex
Carson City, NV 89710

C. H. Johnson, Technical
Program Manager
Nuclear Waste Project Office
State of Nevada
Capitol Complex
Carson City, NV 89710

John Fordham
Desert Research Institute
Water Resources Center
Post Office Box 60220
Reno, NV 89506

Dr. Martin Mifflin
Desert Research Institute
Water Resources Center
Suite 201
1500 East Tropicana Avenue
Las Vegas, NV 89109

Department of Comprehensive
Planning
Clark County
225 Bridger Avenue, 7th Floor
Las Vegas, NV 89155

Planning Department
Nye County
Post Office Box 153
Tonopah, NV 89049

Lincoln County Commission
Lincoln County
Post Office Box 90
Pioche, NV 89043

Economic Development
Department
City of Las Vegas
400 East Stewart Avenue
Las Vegas, NV 89101

Community Planning and
Development
City of North Las Vegas
Post Office Box 4086
North Las Vegas, NV 89030

J. L. Younker (15)
Science Applications, Inc.
2769 S. Highland Drive
Las Vegas, NV 89101

Dr. William D. Hustrulid
Mining Department
Colorado School of Mines
Golden, CO 80401

6300 R. W. Lynch
6310 T. O. Hunter
6310 NNWSICF
6311 L. W. Scully
6311 L. Ferrine (2)
6312 F. W. Bingham
6313 J. R. Tillerson
6314 G. K. Beall
6314 R. M. Robb (5)
6314 R. E. Stinebaugh
6332 WMP Library
6430 N. R. Ortiz
3141 C. H. Ostrander (5)
3151 W. L. Garner (3)
8024 H. A. Pound
DOE/TIC (28)
(3154-3 C. H. Dalin)